Universidade do Minho
Escola de Medicina

Sónia Maria Barros Carvalho

Targeting glycolysis in *Leishmania* therapy

janeiro de 2023

Sónia Maria Barros Carvalho **Targeting glycolysis in *Leishmania* therapy**

UMinho | 2023

Universidade do Minho
Escola de Medicina

Sónia Maria Barros Carvalho

Targeting glycolysis in *Leishmania* therapy

Dissertação de Mestrado
Mestrado em Ciências da Saúde

Trabalho efetuado sob a orientação de
Doutor Ricardo Jorge Leal Silvestre

janeiro de 2023

AGRADECIMENTOS

Gostaria de agradecer em primeiro lugar ao meu orientador, Doutor Ricardo Silvestre, por me permitir desenvolver este trabalho e por toda a orientação, incentivo e apoio durante a realização do mesmo.

À Carolina, por todo o conhecimento científico e laboratorial transmitido.

À Ana, por toda a ajuda e paciência desde o primeiro dia, assim como todas as chamadas de atenção que me permitiram crescer enquanto pessoa e profissional.

À Marta, pelo apoio, companheirismo laboratorial e discussões científicas que contribuiram para o desenvolvimento deste trabalho.

À Stephanie, por ser a minha "irmã" brazileira e por me mostar uma perspetiva diferente da vida.

À Ana, Marta, Stephanie, Consuelo, Tiago, Ana, Joana, Jorge, Matheus e Ehsan pelos bons momentos vividos dentro e fora do laboratório.

À Agostinha e à Denise pela partilha de vivências e por serem os meus anjinhos salvadores em muitas peripécias.

A todos os elementos do Domínio da Microbiologia e Infeção pelo convívio e partilha de conhecimento científico na área de imunologia.

Aos meus pais e ao meu irmão por todo o carinho e apoio incondicional desde sempre.

Aos meus familiares mais próximos por me apoiarem ao longo desta jornada.

A Deus, por Tudo.

FINANCIAL SUPPORT

The work presented in this thesis was performed in the Life and Health Sciences Research Institute (ICVS), University of Minho. Financial support was provided by National funds, through the Northern Portugal Regional Operational Programme (NORTE 2020), under the Portugal 2020 Partnership Agreement, through the European Regional Development Fund (FEDER) (NORTE-01-0145-FEDER-000013) and through the Foundation for Science and Technology (FCT) – projects UIDB/50026/2020, UIDP/50026/2020, PTDC/CVT-CVT/4808/2020 and contract CDDCIND/00185/2020 to RS.

STATEMENT OF INTEGRITY

I hereby declare having conducted this academic work with integrity. I confirm that I have not used plagiarism or any form of undue use of information or falsification of results along the process leading to its elaboration.

I further declare that I have fully acknowledged the Code of Ethical Conduct of the University of Minho.

A glicólise como alvo imunoterapêutico adjuvante contra a *Leishmania*

Resumo

A leishmaniose visceral (LV) é uma doença parasitária transmitida por vetores que pode ser fatal se não for tratada. Embora estejam disponíveis várias terapias contra a *Leishmania*, os problemas associados de eficácia, resistência emergente e toxicidade, requerem abordagens imunoterapêuticas inovadoras. A interação metabólica hospedeiro-patógeno é crucial para o resultado da infeção, definindo a evasão microbiana e as estratégias de proteção do hospedeiro.

Observamos anteriormente que a glicólise serve como a principal fonte de energia para as funções antileishmanicidas contra a LV, e a inibição desta via resultou num aumento da suscetibilidade do hospedeiro, associada a um aumento da carga parasitária aguda. Exploramos aqui o impacto da ativação da glicólise no contexto de infeção da LV. Para tal, realizamos um rastreio de fármacos conhecidos por ativarem a glicólise, analisando a capacidade dos fármacos de induzirem a eliminação do parasita em culturas *in vitro* de macrófagos derivados de medula óssea infetados com *L. donovani*. Entre os diversos fármacos indutores de glicólise testados, a meclizina, um antagonista do recetor H1 da histamina comumente aplicado na clínica, demonstrou ser o mais eficaz na redução da carga parasitária aguda de uma forma dose-dependente. Demonstrou-se que a meclizina induz uma redução significativa da carga parasitária aguda com doses a partir dos 10 μM, mas apenas promove a polarização dos macrófagos para o tipo M1 com doses próximas de 50 μM. Esta diferença de doses demonstrou ser parcialmente explicada pela toxicidade direta da meclizina para o parasita axénico e possivelmente pelo conhecido efeito da meclizina em diferentes vias metabólicas do hospedeiro de relevância no contexto da inflamação.

Dados preliminares mostram um efeito sinérgico entre a meclizina e a miltefosina (única terapia anti-*Leishmania* disponível oralmente) na redução da carga parasitária aguda *in vitro*. Experiências futuras desvendarão o mecanismo de ação da meclizina e a importância do aumento da glicólise na resposta imunitária do hospedeiro, com o consequente controlo da carga parasitária intracelular. Globalmente, isto permitir-nos-á abordar um possível adjuvante imunoterapêutico para a eficácia da terapêutica anti-*Leishmania* de primeira linha atualmente existente.

Palavras-chave: Glicólise; Imunometabolismo; Leishmaniose Visceral; Macrófago; Meclizina

Targeting glycolysis in *Leishmania* therapy

Abstract

Visceral Leishmaniasis (VL) is a vector-borne parasitic disease, fatal if untreated. Although several available anti-*Leishmania* therapies are described, the associated efficacy problems, emerging drug resistance and toxicity require innovative immunotherapeutic approaches. The host-pathogen metabolic interaction is crucial for the outcome of infection, defining microbial evasion and host protective strategies.

We have previously observed that glycolysis serves as the major energy source for antileishmanial effector functions against VL, and the inhibition of this pathway resulted in increased host susceptibility, associated with increased acute parasite load. Here, we explored the impact of activating glycolysis in the VL infection context. For that, we performed a drug screening of compounds known to activate glycolysis, analysing the drug-induced parasite clearance in *in vitro* cultures of *L. donovani*-infected bone marrow-derived macrophages. Among the distinct glycolysis-inducing drugs tested, meclizine, a histamine H1-receptor antagonist commonly applied in the clinic, has been shown to be the most effective in reducing the acute parasite load in a dose-dependent manner. Meclizine has been shown to induce a significant reduction in the acute parasite load at doses starting at 10 μM, but only promotes the M1-like macrophage polarization with doses near 50 μM. This dose difference was shown to be partially explained by the direct meclizine's toxicity to the axenic parasite and possibly by the known effect of meclizine in different host metabolic pathways of relevance in the context of inflammation.

Preliminary data showed a synergistic effect between meclizine and miltefosine (the only anti-*Leishmania* therapy orally available) in reducing the acute parasite load *in vitro*. Future experiments will unfold the mechanism of action of meclizine and the importance of glycolysis enhancement on host immune response and consequent control of the intracellular parasite load. Overall, this will allow us to address a possible immunotherapeutic adjuvant for the existing first-line anti-*Leishmania* therapeutics efficacy.

Keywords: Glycolysis; Immunometabolism; Macrophage; Meclizine; Visceral Leishmaniasis

INDEX

Agradecimentos ... iii

Financial Support ... iii

Resumo ... v

Abstract ... vi

Index ... vii

List of Abbreviations ... ix

List of Figures ... xii

List of Tables ... xiii

Introduction ... 1

I.1. Leishmaniasis ... 1

I.2. Actual treatments ... 2

I.3. *Leishmania spp.* life cycle ... 4

I.4. Mammalian host-parasite interaction and associated host metabolism ... 6

I.4.a. Innate immune system ... 6

I.4.b. Adaptive immune system ... 10

I.5. Host glycolysis in the visceral leishmaniasis context ... 12

Research Objectives ... 15

Materials and Methods ... 16

M.1. Mice and Ethics Statement ... 16

M.2. Primary Murine Bone Marrow-Derived Macrophages ... 16

M.3. Axenic *L. donovani* cultures ... 17

M.3.a. *L. donovani* culture maintenance ... 17

M.3.b. *L. donovani* toxicity assay ... 17

M.4. *In vitro* infection and treatments ... 17

M.5. *In vivo* infection, treatments, and necropsy ... 17

M.6. Parasite Rescue and Transformation Assay ... 18

M.7. Sulforhodamine B Assay ... 19

M.8. High-Performance Liquid Chromatography ... 19

M.9. Flow Cytometry ... 20

M.10. Enzyme-Linked Immunosorbent Assay ... 21

M.11. RNA extraction and complementary DNA synthesis 21
M.12. DNA extraction 21
M.13. Real-time quantitative polymerase chain reaction 22
M.14. Statistical Analysis 22
Results 24
R.1. Drug Screening 24
R.2. Meclizine dose-response of infected macrophages 28
R.3. Meclizine dose-response of axenic *L. donovani* cultures and non-infected macrophages 32
R.3.a. Axenic *L. donovani* cultures 32
R.3.b. Meclizine dose-response of non-infected macrophages 33
R.4. Mechanism of action of Meclizine 36
R.5. Meclizine as an adjuvant to Miltefosine 38
R.6. Effect of Meclizine *in vivo* 40
Discussion 44
Concluding Remarks and Future Perspectives 49
References 50
Annex 62

LIST OF ABBREVIATIONS

3PO – Trimethyl Phosphate

AKT – Protein Kinase B

AmB – Amphotericin B

AMP – Adenosine Monophosphate

APCs – Antigen-Presenting Cells

ATP – Adenosine Triphosphate

BMDMs – Bone Marrow-Derived Macrophages

CD – Cluster of Differentiation

CI – Confidence Interval

CL – Cutaneous Leishmaniasis

CO_2 – Carbon Dioxide

cRPMI – Complete RPMI (*supplemented medium*)

DMEM – Dulbecco's Modified Eagle Medium

DMOG – Dimethyloxalylglycine

DMSO – Dimethyl Sulfoxide

DNA – Deoxyribonucleic Acid

ELISA – Enzyme-Linked Immunosorbent Assay

FBS – Foetal Bovine Serum

GAPDH – Glyceraldehyde-3-Phosphate Dehydrogenase

H1R – Histamine H1 Receptor

HEPES – 4-(2-Hydroxyethyl)-1-Piperazineethanesulfonic Acid

HIF – Hypoxia-Inducible Factor

HIV – Human Immunodeficiency Virus

HPLC – High-Performance Liquid Chromatography

HSCs – Hematopoietic Stem Cells

IC_{50} – Half Maximal Inhibitory Concentration

IL – Interleukin

INF-γ – Interferon-γ

iNOS – Inducible Nitric Oxide Synthase

M-CSF – Macrophage Colony-Stimulating Factor

MCL – Mucocutaneous Leishmaniasis

MHC – Major Histocompatibility Complex

mTOR – Mammalian Target of Rapamycin

NAD^+ – Nicotinamide Adenine Dinucleotide (*oxidized form*)

NADPH – Nicotinamide Adenine Dinucleotide Phosphate (*reduced form*)

NETs – Neutrophil Extracellular Traps

NO – Nitric Oxide

P:C:I – Phenol:Chloroform:Isoamyl Alcohol

PBS – Phosphate Buffer Saline

PCYT2 – CTP:Phosphoethanolamine Cytidylyltransferase

PCR – Polymerase Chain Reaction

Pen/Strep – Penicillin-Streptomycin

***per os* –** Oral Gavage

PFA – Paraformaldehyde

PFK – Phosphofructokinase

PFKFB3 – 6-Phosphofructo-2-Kinase/Fructose-2,6-Biphosphatase 3

PGK1 – Phosphoglycerate Kinase 1

PI3K – Phosphatidylinositol-3-Kinase

PK – Pyruvate Kinase

PKDL – Post-Kala-Azar Dermal Leishmaniasis

PPP – Pentose Phosphate Pathway

PRTA – Parasite Rescue and Transformation Assay

PVs – Parasitophorous Vacuoles

qPCR – Quantitative PCR

RNA – Ribonucleic Acid

ROS – Reactive Oxygen Species

RPMI – Roswell Park Memorial Institute (*medium*)

SRB – Sulforhodamine B

T_c – Cytotoxic T (cell)

TCA – Tricarboxylic Acid

TGF – Transforming Growth Factor

T_h – Helper T (cell)

TLR – Toll-Like Receptor

TNF-α – Tumour Necrosis Factor-α

T_{reg} – Regulatory T (cell)

TRMs – Tissue-Resident Macrophages

VL – Visceral Leishmaniasis

WHO – World Health Organization

LIST OF FIGURES

Figure 1. *Leishmania spp.* life cycle. 5
Figure 2. M1 and M2 macrophage polarizations. 10
Figure 3. Glycolytic targets of the tested compounds. 25
Figure 4. Drug screening test *in vitro*. 25
Figure 5. Meclizine presents the highest induced parasite load reduction *in vitro*. 27
Figure 6. Only daprodustat, DMOG and Roxadustat demonstrate an apparent effect on the lactate/glucose ratio. 28
Figure 7. Dose-response of infected macrophages *in vitro*. 29
Figure 8. Meclizine induces a significant parasite burden reduction *in vitro* with doses close to 10 μM, but only promotes a macrophage M1-like polarization with 40 to 50 μM doses. 30
Figure 9. Meclizine induces a dose-dependent impairment in the growth of axenic cultures of *L. donovani* promastigotes. 33
Figure 10. Dose-response of non-infected macrophages *in vitro*. 34
Figure 11. Meclizine induces a M1-like macrophage polarization in *in vitro* non-infected macrophages with 40 to 50 μM doses. 35
Figure 12. Mechanism of action of Meclizine in the *L. donovani*-infected BMDMs *in vitro* model is not through direct modulation of the glycolytic pathway. 37
Figure 13. Meclizine and Miltefosine demonstrate a synergic effect on the intracellular parasite load, with an apparent reduction in the host M2-like phenotype and a possible increase in the M1-like phenotype. 39
Figure 14. Experimental design *in vivo*. 41
Figure 15. Meclizine did not induce a reduction in the organs parasite load nor induced significant changes in the T cells sub-populations percentage. 42

LIST OF TABLES

Table 1. Flow cytometry antibody panel applied in the *in vitro* experiments 20

Table 2. Flow cytometry antibody panels applied in the *in vivo* experiment 20

Table 3. Primers used in the qPCR reactions and respective nucleotide sequences 22

INTRODUCTION

I.1. LEISHMANIASIS

Leishmaniases are vector-borne parasitic diseases caused by intracellular parasites of the genus *Leishmania* [1, 2]. It affects several mammalian species, mainly dogs and humans, being transmitted between mammalian hosts by the bite of infected female sandflies [2, 3]. These vectors are mostly present in tropical and subtropical regions, and despite the prevention and treatment advances, leishmaniasis remains a major Neglected Tropical Disease as defined by the World Health Organization (WHO) [4-7].

According to the *Leishmania* species, sandfly vector, and mammalian host characteristics (primarily its immune response), leishmaniasis can present diverse clinical manifestations, ranging in severity from minor self-healing skin lesions to life-threatening visceral infection [2, 8, 9]. In this manner, it can be divided into four main types: cutaneous leishmaniasis (CL), mucocutaneous leishmaniasis (MCL), visceral leishmaniasis (VL), and post-kala-azar dermal leishmaniasis (PKDL).

CL is the most common form of this disease [7] and is characterized by self-limiting skin ulcers in exposed areas of the skin, that heal within 3-18 months, with the possibility of leaving scars [2, 10]. In 2020, WHO registered 208 357 new CL cases worldwide, with more than 80% being reported in the Middle East and Central Asia (Syrian Arab Republic, Afghanistan, Pakistan, and Iraq), South America (Brazil, Colombia and Peru), and Southern Mediterranean (Algeria and Tunisia) [7]. This clinical form of leishmaniasis can be induced by *Leishmania major*, *L. tropica*, *L. aethiopica*, *L. amazonensis*, *L. mexicana*, *L. braziliensis* and *L. guyanensis*, with species-specific clinical manifestations and geographic distributions [10].

MCL is one type of CL progression and is characterized by the proliferation of skin ulcers to the mucosal tissue of the nose, mouth, and throat, leading to serious disfiguring scenarios caused by an intensive immunopathological response [10, 11]. In this manner, MCL is a life-threatening condition that can take years to recover [10-12]. It can occur in patients infected with *L. braziliensis*, *L. guyanensis* or *L. aethiopica* [12, 13].

VL, also known as kala-azar, is the most severe form of this disease [7] and is characterized by weight loss, fever, anaemia and expansion of the spleen and liver, which leads to hepatosplenomegaly, polyclonal hyper-gammaglobulinemia and immunosuppression [2, 5, 6]. Despite the decline in the number of cases over the last decade, in 2020 WHO registered 12 838 new VL cases worldwide, of which 96% were in the Eastern Mediterranean Region (Sudan, Somalia, Yemen, and Iraq), South-East Asia Region (India, and

Nepal), South America (Brazil), and Africa (Kenya, Ethiopia, Eritrea, South Sudan, and Chad) [7]. Many patients become severely immunocompromised and may become victims of chronic secondary infections, such as tuberculosis, malaria, and human immunodeficiency virus (HIV) infection (extensively reviewed in [14]). The VL/HIV co-infection is a particularly complex clinical condition, being recognized by WHO as a severe obstacle in the treatment of these patients [7]. Due to the detrimental synergy between these two pathologies, the host immune system is severely weakened, and VL/HIV patients can present a more developed clinical onset and increased mortality (reviewed in [15-18]). Overall, due to the severe systemic conditions, VL is fatal within 2 years if left untreated [2, 7, 19]. Between 2014 and 2020, WHO registered 3813 deaths, of which 89% were among new cases [7]. This type of disease is caused by the anthroponotic *L. donovani* in humans, mainly in India and sub-Saharan Africa, and by the zoonotic *L. infantum* (humans and dogs), mainly in southern Europe, North Africa, and Brazil, with rare cases induced by *L. tropica* [2, 20].

PKDL is a skin condition that arises upon recovery of VL infections induced by *L. donovani* and is due to persistent parasites in the skin [7, 21]. PKDL skin lesions self-heal within 1 year, presenting a reduced risk to the patient [21]. However, if untreated, these are *L. donovani* reservoirs easily accessible for sandflies, increasing the risk of transmission and the possibility of new VL cases arousal in the region [7, 21]. In 2020, 778 PKDL cases were registered by WHO, of which 96% were in India [7].

Considering that between the different types of leishmaniasis, VL is the clinical form with more associated complications and with the highest risk of death, it was the pathology chosen for the focus of this study.

I.2. ACTUAL TREATMENTS

Currently, there is no vaccine against VL, so the treatment relies solely on the available chemotherapies. However, due to their efficacy problems, emerging drug resistance, and toxicity, there is a need for the development of new therapeutical approaches, crucial for patients survival [6]. Furthermore, considering that most people affected by this disease live in poverty, the high cost of treatments and the need for hospitalization means that many patients do not complete their current treatment [22]. In the case of VL/HIV co-infected patients, the suppression of the immune system makes it even more difficult to apply some of the VL standard treatments, due to the patients' unresponsiveness to these therapies [18, 23].

Pentavalent Antimonials

For decades, VL was treated with pentavalent antimonials monotherapy – the first therapy available. However, due to parasite resistance, the response to these compounds began to vary significantly between regions, with an effectiveness rate between 35% in India and 95% in other countries [24, 25]. In addition, side effects such as cardiac arrhythmias and tachycardia, and painful muscular injections for 30 days, led to the search for other compounds [26].

Amphotericin B

Amphotericin B (AmB) was recommended for patients with pentavalent antimonials resistance, being used as a first-line drug in India [27, 28]. It presented excellent efficacy (~100%) and high safety with intravenous injections [29]. However, adverse reactions arose, such as fever, toxicity, and the need for prolonged hospitalization with close monitoring of renal functions [30].

Lipid formulations of AmB

The later administration of AmB complexed in liposomes reduced its toxicity and provided a safer and highly effective alternative [28, 30]. There are currently six different lipid formulations available, with different doses, efficacies, and toxicities. Among these, Ambisome® proves to be one of the most effective anti-*Leishmania* treatments available, but its high cost is still the main obstacle [28, 31, 32].

Pentamidine

Upon AmB treatment, pentamidine was recommended as a second-line treatment for pentavalent antimonials resistant VL patients. Compared to AmB, it has a reduced cure rate and toxicity problems [33]. However, it is recommended as secondary prophylaxis for VL/HIV co-infection patients [17, 34, 35].

Paromomycin

Paromomycin is an inexpensive broad-spectrum antibiotic with activity against diverse gram-positive and gram-negative microorganisms, mycobacteria, and protozoa [30]. It demonstrated a high anti-leishmanial efficacy (~98%) either as a monotherapy or when combined with sodium stibogluconate (pentavalent antimonial), being well tolerated by VL patients [36, 37]. The adverse effects include pain at the injection site, fever, proteinuria, an increase in bilirubin and alkaline phosphatase values, and vomiting [30].

Miltefosine

Miltefosine was the first effective (~94%) oral treatment against VL, being licenced for use in India, Germany, Colombia, and Bangladesh [38]. Its oral administration made domestic treatment feasible. However, there is no control over the compliance for the 28 days of treatment by patients. Furthermore,

it has a half-life of 7 days in humans and may give rise to the development of parasite resistance [30, 39].

Combined therapies

Considering that each of these compounds has serious disadvantages, especially due to long periods of treatment to be effective as monotherapies, there has been an investment in recent years in the development and application of combined therapies [40, 41]. Among the diverse combined regimes that had been developed, (1) intravenous injections of 4 mg/Kg/day of pentamidine three times a week until parasitological cure + intramuscular injections of 20 mg/Kg/day of sodium stibogluconate for 20 days; (2) a single intravenous injection of 5 mg/Kg of liposomal AmB + oral administration of 50 mg/day of miltefosine for 7 days; and (3) intramuscular injections of 11 mg/Kg/day of paromomycin for 10 days + oral administration of 50 mg/day of miltefosine for 10 days, represented three effective treatment options, with a definite cure rate of 98-99% [42, 43]. This has significantly reduced the time and cost of treatments, increased their effectiveness, reduce toxic effects, and slowed the emergence of parasite resistance (reviewed in [30, 40, 41]). Furthermore, immune-based therapies in combination with the currently applied chemotherapies, that boost the immune system response, may represent an interesting approach in the treatment of VL patients, as has been recently observed in other studies [44-46].

I.3. *LEISHMANIA SPP.* LIFE CYCLE

Leishmania spp. have a heterogenous life cycle, with two different morphological stages that interchange along the path between its hosts: sandflies and mammals. In the digestive tract of an infected female sandfly, *Leishmania spp.* is found in its flagellated mobile form, known as promastigote. In this form, it multiplies through binary fission, colonising the thoracic and abdominal midguts of the sandfly [47]. As it moves towards the sandfly foregut, *Leishmania* promastigotes continue to replicate and acquire characteristics that allow them to already survive in the mammalian host, thus being in their most infectious stage [47].

During an infected sandfly blood meal, promastigotes are injected into the mammalian host skin, being phagocytosed by different innate immune cells (discussed in more detail in **I.4.**) [47, 48]. Once inside the mammalian host, *Leishmania spp.* preferentially colonise macrophages, where they differentiate into obligatory intracellular amastigotes, inside parasitophorous vacuoles (PVs) [5, 49]. These PVs are mature acidified phagolysosomes (pH 5.5) and result from a dynamic fusion between host vesicles (phagocytic, endocytic, autophagic and endoplasmic reticulum vesicles), providing a wide range of sugars, lipids, and amino acids, that can be taken by amastigotes, allowing its intracellular survival

(reviewed in [50-52]). Amastigotes are ovoid and non-flagellated, which increase in number by binary fission, leading to subsequent host cell's bursting and infection of other cells, propagating infection [53].

When a female sandfly searches for a blood meal, it inserts its saw-like mouthparts into the mammalian host skin, producing a small wound. Here, blood from capillaries flows into the sandfly gut, carrying infected macrophages (recruited due to tissue damage) or recently released amastigotes, present in the skin [48]. The differences in the environment when the parasite is transferred from the mammalian host to the sandfly gastrointestinal tract (decreased temperature and increased pH) trigger morphological changes in the amastigote, converting into its promastigote form, restoring the cycle (**Figure 1**) [48, 54].

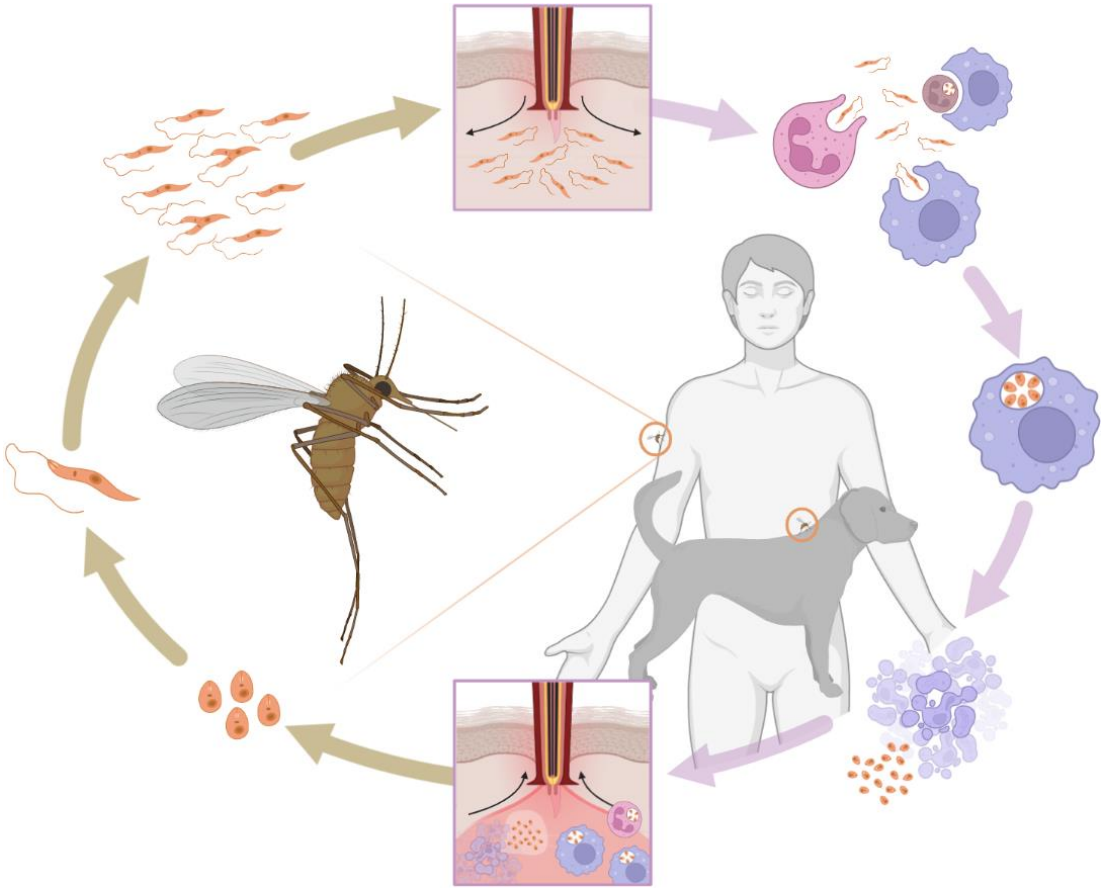

Figure 1. *Leishmania spp.* life cycle. *Leishmania spp.* is found in its flagellated mobile form (promastigote) inside the digestive tract of infected female sandflies. Here, promastigotes multiply by binary fission and acquire infectivity characteristics, that allow them to survive inside the mammalian host. During a sandfly blood meal, *Leishmania* promastigotes are injected into the mammalian host skin and are phagocytosed by different innate immune cells. However, *Leishmania spp.* preferentially colonise macrophages, where they differentiate into obligatory intracellular amastigotes inside parasitophorous vacuoles. Amastigote proliferation leads to subsequent host cell bursting and can infect other host cells, propagating infection. Later, in another sandfly blood meal, infected macrophages, recently released amastigotes, and other infected cells are transferred to the sandfly digestive tract, where the different environmental characteristics trigger the amastigote conversion to promastigote, restoring the cycle of infection. Schematic representation created with BioRender (app.biorender.com).

I.4. MAMMALIAN HOST-PARASITE INTERACTION AND ASSOCIATED HOST METABOLISM

The host immune system has several mechanisms that confer protection against different invading pathogens without compromising the integrity of the host itself [55, 56]. It can be divided into innate and adaptive immune system responses, and the cooperation between cells of these two types of response is essential for an effective and protective anti-*Leishmania* response. On the other hand, *Leishmania spp.* have evolved and developed strategies to escape the host's immune response and promote their intracellular survival, with consequent maintenance of chronic infections [57].

I.4.a. Innate immune system

The innate immune system is responsible for the immediate, less specific response to any invading agent, being constituted by physical barriers (i.e., skin and mucous membranes), chemical barriers (e.g., antimicrobial peptides and reactive oxygen species (ROS)), complement system, innate antibodies, and by cells derived from the differentiation of hematopoietic stem cells (HSCs) in the bone marrow [55, 56]. These cells present diverse functions essential for the primary defence against pathogens. According to their germline, which partially defines their functions and morphological characteristics, innate immune cells can be divided into non-myeloid cells, myeloid cells, and some lymphoid cells [56]. However, in this section, we will focus on the main cells involved in the response against *Leishmania* – neutrophils and macrophages, which belong to the myeloid germline. These express pattern recognition receptors (PRRs) that recognize pathogen-associated molecular patterns (PAMPs) and host cells' damage-associated molecular patterns (DAMPs) [56].

Neutrophils

Once injected into the mammalian host skin, *Leishmania* promastigotes are initially phagocytosed by neutrophils, the first cell type recruited from the blood stream to the site of infection [48, 56, 57]. The primary function of these cells is to enter injury sites, attracted by chemotactic factors and cytokines (derived from the host tissue, sandfly saliva, or the parasite), and initiate an immediate parasite clearance [56, 57]. This can happen through the formation and engulfment into the phagosome where ROS will kill the parasite; or by the breakdown of the neutrophils' nuclear content and consequent release to the extracellular environment as neutrophil extracellular traps (NETs), with the secretion of toxic compounds [58-60]. This process can be ROS-dependent or independent, with the first leading to consequent neutrophil death through a process called NETosis [60, 61]. In VL patients, neutrophils are highly activated [62], but the VL-inducing *Leishmania* species – *L. donovani* and *L. infantum*, have been shown

to survive NETs *in vitro* and in humans [63, 64], which may be indicative of these parasites escape from neutrophils' immunity [65].

When activated in the context of infection, neutrophils present a rapid pro-inflammatory response, which requires large amounts of adenosine triphosphate (ATP) in a short time [66]. Thus, activated neutrophils are highly dependent on glycolysis to obtain energy and the subsequent pyruvate lactic fermentation to regenerate the oxidized nicotinamide adenine dinucleotide (NAD^+) levels, essential for the maintenance of the glycolytic pathway [67]. In this manner, neutrophils present few mitochondria, reduced oxygen consumption, and increased glycolytic pathway through a mechanism similar to the Warburg effect, with increased activity in the pentose phosphate pathway (PPP) [68, 69]. The increase in the PPP activity leads to the synthesis of the reduced form of nicotinamide adenine dinucleotide phosphate (NADPH), which is also extremely important for the pro-inflammatory response of neutrophils. NADPH is used in the production of antioxidant molecules (i.e., glutathione) and through the NADPH oxidase it produces superoxide free radicals, a type of ROS [70].

However, *Leishmania spp.* evolved to survive inside neutrophils. *L. donovani* promastigotes present surface glycolipids, such as lipophosphoglycan, that inhibit phagosome fusion with lysosomes, protecting them from ROS, enzymes, and antimicrobial peptides-induced degradation [71]. In addition, *L. donovani* can attract neutrophils to the infection site, and the interaction with these leads to the inhibition of interferon-γ (INF-γ)-induced protein 10 (IP-10) production (involved in natural killer cells activation) and induces the production and release of interleukin (IL)-8, which promotes the attraction of more neutrophils [72]. Furthermore, *Leishmania spp*. increase infected neutrophils survival, and with the inhibition of their parasite-killing properties, *Leishmania spp.* take over neutrophils and uses them as "Trojan horses" to be phagocytosed by macrophages – their host cell of choice [73, 74].

Macrophages

Macrophages are antigen-presenting cells (APCs) that, in addition to providing a rapid response against invading pathogens, can establish a connection with cells of the adaptative immune system, promoting and maintaining an adaptative immune response against the same pathogens [55, 57].

Macrophages are a very heterogeneous population, according to their germ lineage, location in tissues and functions performed. In general, these can be divided into tissue-resident macrophages (TRMs) and inflammatory monocyte-derived macrophages [56, 75]. TRMs are tissue-specific macrophages with microanatomical-specific functions, essential for the maintenance of tissue homeostasis [75]. Furthermore, according to external and internal stimuli, TRMs can alter their metabolism, and

consequently their tissue functions to (1) act as immune sentinels, providing a rapid first-line response to invading pathogens and transmitting information to other cells of the immune system; (2) act as tissue housekeepers, removing debris, apoptotic cells, unwanted molecules and/or microorganisms; or (3) act as anti-inflammatory tissue healing agents (reviewed in [75, 76]). On the other hand, monocyte-derived macrophages are originated from bone marrow HSCs and are differentiated into macrophages upon recruitment of bloodstream circulating monocytes to the site of inflammation [56]. In response to different stimuli, monocyte-derived macrophages (and some TRMs) can be activated, and considering the plasticity of these cells, macrophages can present a continuous spectrum of phenotypes, ranging from the classically activated pro-inflammatory M1 phenotype, with potent microbicidal activity, to the alternative activated M2 phenotype, associated with tissue healing and anti-inflammatory properties, which antagonizes the M1 phenotype response (reviewed in [5, 77-79]).

The development of a protective anti-*Leishmania* immune response, essential for parasite killing, is associated with an IFN-γ- and PRRs agonists-induced macrophage polarization to a pro-inflammatory M1-like phenotype [5, 80, 81]. It is characterized by intracellular stimulation of the inducible nitric oxide (NO) synthase (iNOS) and NADPH oxidase 2, with consequent increase of the NO and ROS levels, respectively. This leads to parasite clearance and secretion of inflammatory cytokines, such as tumour necrosis factor-α (TNF-α), IL-6 and IL-12 [5, 57, 79-82]. This is the primary macrophage response following *Leishmania* infection that contribute to promote a T helper (T_h)1 immune response [5, 56, 79, 80, 82]. This phenotype relies mainly on glycolysis to sustain the rapid ATP requirements even in low oxygen availability, as may occur in inflammation sites; and on PPP for NO production [83, 84]. Also, increased activity of glycolytic enzymes such as glyceraldehyde-3-phosphate dehydrogenase (GAPDH) and pyruvate kinase (PK) 2 induce the production of TNF-α and IL-1β by macrophages, which attracts macrophages and induce their M1-like polarization [84]. Furthermore, M1-like macrophages present a partially blocked tricarboxylic acid (TCA) cycle, which contributes to IL-1β and NO production, by an accumulation of the TCA cycle intermediates succinate and citrate, used in their synthesis [85]. The M1-like phenotype is schematized in **Figure 2**.

To survive under these extreme conditions, *Leishmania* promastigotes differentiate into amastigotes, which present a more quiescent metabolism, reduced growth rate and stringent metabolic response [49, 51, 86, 87]. This latter confers them protection against exposure to host cells' NO and ROS [88]. Also, despite having access to different carbon sources within the PVs, amastigotes reduce their expression of glucose and amino acids transporters and become more dependent on oxidative phosphorylation for their ATP synthesis from the adenosine monophosphate (AMP) pool [51]. In addition, their TCA cycle is

truncated, being primarily used for amino acids synthesis [88]. However, *Leishmania spp.* are auxotrophic for several essential nutrients, such as purines, amino acids, carbon sources, and vitamins, that must be scavenged from the macrophage [50, 51]. For instance, *Leishmania spp.* are completely dependent on host arginine levels for their synthesis of proteins and essential metabolites (e.g., polyamines, trypanothione and hypusine) [89-92]. Polyamines are key regulators in parasite growth and differentiation, and are crucial for their antioxidant defence by trypanothione, which is a specific parasite derivative of host polyamines [89, 91, 92]. Also, the levels of arginine and its downstream metabolites are reduced inside the PVs, and the modulation of macrophage arginine levels can enhance or limit parasite growth [93]. In this manner, amastigotes need to compete against the macrophage for the available arginine, by the *Leishmania* arginine transporters present in their cell membrane and PVs [89, 90, 93, 94]. Furthermore, *Leishmania* can modulate host gene expression, with the most differently regulated pathways being associated with immune response signalling and apoptosis [95, 96]. However, different genes are expressed during the different stages of parasite development [90, 96], and are dependent on the host's genetic susceptibility [95, 97].

With these mechanisms, *Leishmania* parasites can resist the M1-like pro-inflammatory response and push forward a pro-survival M2-like phenotype [98, 99]. In this manner, infected macrophages become permissive parasite reservoirs and promote their proliferation [98, 99]. These *Leishmania*-induced M2-like macrophages can be maintained even under a strong host-induced pro-inflammatory stimulus, by local feedback loops and excessive NO secretion, which hinders the inflammatory response [5].

Macrophages with a M2-like phenotype are also naturally present in tissues, especially in sites of injury or infections, being associated with tissue healing, anti-inflammatory properties and immunoregulatory effect, with induction of a T_h2 immune response [5, 77-79]. This macrophage polarization is induced by anti-inflammatory cytokines, such as IL-4, IL-10, and IL-13, and is characterized by reduced glycolysis, increased mitochondrial oxidative phosphorylation, and stimulation of a fully functional TCA cycle, providing efficient ATP production [79, 80, 99-102]. M2-like macrophages secrete anti-inflammatory cytokines, such as IL-10, transforming growth factor (TGF)-β, and IL-1 receptor antagonist (reviewed in [79, 80, 100]). The M2-like phenotype is schematized in **Figure 2**.

Changes in macrophage polarization lead to significant changes in the intracellular arginine levels. M1-like macrophages have increased levels of arginine due to the increased expression of arginine transporter and iNOS, which converts the arginine into citrulline and NO, essential for parasite elimination [89, 103, 104]. In turn, M2-like macrophages, have increased expression of arginine transporters and upregulation of arginase-1. This enzyme hydrolases arginine to ornithine, which is a precursor for the *de*

novo synthesis of glutamine, proline, and polyamines, sustaining the tissue repairing functions [89, 102, 105]. Arginase-1 diverts arginine from the NO production and is also inversely regulated with iNOS, leading to reduced macrophage antileishmanial functions and increased parasite survival [93, 104].

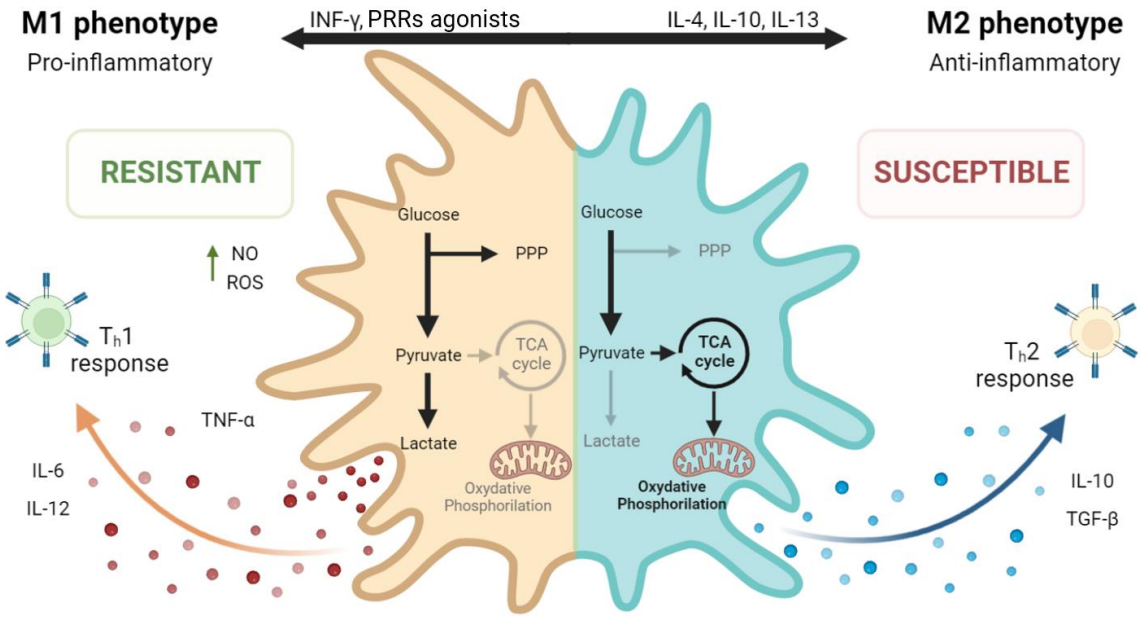

Figure 2. M1 and M2 macrophage polarizations. The M1-like macrophage phenotype is characterized by a pro-inflammatory response, with a glycolytic metabolism followed by lactate fermentation, and high levels of nitric oxide (NO) and reactive oxygen species (ROS), that control the parasite load. Both the pentose phosphate pathway (PPP) and the truncated tricarboxylic acid (TCA) cycle, alongside the inducible NO synthase (iNOS) and nicotinamide adenine dinucleotide phosphate (NADPH) oxidase, contribute to the increased NO and ROS levels. M1-like macrophages secrete pro-inflammatory cytokines such as tumor necrosis factor-α (TNF-α), IL-6 and IL-12, activate T cells and induce the T helper 1 (T_h1) response. This M1 macrophage polarization is induced by interferon-γ (INF-γ) and pattern recognition receptors (PRRs) agonists. On the contrary, the M2-like macrophage phenotype is characterized by a tissue-healing-associated anti-inflammatory response, with a metabolic preference for oxidative phosphorylation. This phenotype is associated with a permissive *Leishmania* reservoir and favours the intracellular parasite survival. M2-like macrophages secrete anti-inflammatory cytokines such as IL-10 and transforming growth factor-β (TGF-β) and induce the T_h2 adaptive immune response. This M2 macrophage polarization is induced by IL-4, IL-10 and IL-13, as well as *Leishmania* factors. Schematic representation created with BioRender.

I.4.b. Adaptive immune system

The adaptive immune system is mainly composed of lymphoid cells that upon activation, provide a specific and long-lasting response against specific antigens [56]. Among the adaptive immune cells, B and T cells are the two major cell types involved in response against *Leishmania spp.* [106-108], but in the context of this master thesis, we will focus only on the T cells.

T cells

T cells derive from bone marrow HSCs and only complete their maturation in the thymus after a process of positive and negative selection by the APCs [107]. T cells have specific T cell receptors in their surface membrane that recognize the corresponding major histocompatibility complex (MHC) presented by the APCs [107, 108]. In a context of *Leishmania* infection, the MHC complex displays the parasite-associated antigen, priming naïve T cell activation to induce the correspondent antigen-specific response [107, 108]. According to the initial APCs stimulus, T cells can differentiate into T_h cells, regulatory T cells (T_{reg} cells) or cytotoxic T cells (T_c cells) [108]. Considering that T_h, T_{reg}, and T_c cells have a strong interaction with the cells of the innate immune system, we will focus on their role in the context of *Leishmania* infection and in regulating the innate and adaptive immune response.

Helper T cells

T_h cells present in their surface membrane the glycoprotein CD4 (cluster of differentiation 4) and can only be activated by MHC class II complexes. Upon this activation, and according to the microenvironment, T_h cells became active effector T cells and can be divided into the T_h1, T_h2 and T_h17 subsets [108, 109].

T_h1 cells secrete the pro-inflammatory cytokines IL-12, INF-γ and TNF-α and sustain the pro-inflammatory immune response, with activation of macrophages iNOS (by INF-γ) and consequent increase of NO production, promoting the M1-like phenotype and infection control [5, 109, 110]. This pro-inflammatory T_h1 response is important in the effective control of parasite load, with its inhibition *in vivo* leading to increased host susceptibility and higher parasite load [111, 112]. T_h17 cells work in synergism with the T_h1 INF-γ response, increasing macrophage NO production, and promoting neutrophil recruitment to the site of infection [113, 114]. T_h1 and T_h17 are induced by pro-inflammatory innate immune cells stimuli, such as IL-1β, IL-6, IL-12, IL-18 and IL-23 cytokines and toll-like receptors (TLRs) like TLR2, TLR7, TLR8 and TLR9 [1, 108, 115].

In opposition, IL-4, IL-10, and IL-13 induce the naïve $CD4^+$ T cells differentiation into T_h2 cells, being associated with host susceptibility, parasite survival and proliferation, and disease progression [109, 116, 117]. T_h2 cells secrete IL-4 and IL-13, which promote the macrophage M2-like phenotype, inducing the production of IL-10, increase arginase-1 expression, and inhibits INF-γ production, resulting in *Leishmania* proliferation and maintenance of chronic infection [100, 107, 118].

During activation, T_h cells upregulate their Warburg-like glycolytic metabolism, to sustain their rapid and extensive proliferation [119-121]. However, only T_h1 and T_h17 cells maintain this glycolytic metabolism after activation since the glycolytic activity is essential for the maintenance of the pro-

inflammatory response of these cells [120-122]. In T_h1 cells, GAPDH recruitment for glycolysis is essential for INF-γ production, since under steady-state conditions GAPDH is bounded to INF-γ messenger ribonucleic acid (RNA), repressing its translation [121, 122]. In T_h17 cells, increased glycolysis leads to increased IL-17 production, and contributes to T_h17 phenotype development [120, 121]. In contrast, T_h2 cells shift to a metabolism more dependent on lipid oxidation, which is consistent with T_h2 anti-inflammatory functions [123].

The T_h1/T_h2 dichotomy has been recognized as an important regulator of host resistance/susceptibility to infection, and cells of the innate immune system are highly susceptible to this T_h1/T_h2 regulation, a feature that *Leishmania* evolved to control [100, 117, 118].

Regulatory T cells

T_{reg} cells are a subgroup of $CD4^+$ T cells whose main function is to suppress the immune system response, prevent autoimmune diseases, allergies, and maintenance of self-tolerance [108]. T_{reg} cells secrete IL-10 and TGF-β and are associated with increased susceptibility to infection [124]. This IL-10 secretion leads to the differentiation and proliferation of T_h2 cells and promotes the M2-like phenotype of macrophages, amplifying the host's anti-inflammatory immune response [100, 117]. Thus, the regulation of T_{reg} and T_h17 populations is crucial in maintaining the host immune response balance [125, 126]. This is achieved through the IL-6 and TGF-β levels, with high IL-6 levels and lower TGF-β levels promoting the T_h17 population, while higher TGF-β levels, combined with other regulatory cytokines, in the absence of IL-6 promote the T_{reg} activity [108, 125, 126].

In contrast to T_h cells, T_{reg} cells are highly dependent on lipid oxidation, presenting a more oxidative metabolism with reduced glycolytic activity, which precedes their immunosuppressive functions [119].

Cytotoxic T cells

Unlike T_h and T_{reg} cells, T_c cells are effector T cells that express the CD8 glycoprotein, being activated by the MHC class I complex [108]. Once activated, T_c cells secrete cytotoxic granules like granzyme and perforin, secrete the pro-inflammatory cytokines INF-γ and TNF-α and disrupt the infected cells, inducing the target cell apoptosis [127]. Similar to T_h cells, once activated, T_c cells have an increased Warburg-like glycolytic activity, promoting their differentiation, proliferation and cytotoxic activity [128].

I.5. HOST GLYCOLYSIS IN THE VISCERAL LEISHMANIASIS CONTEXT

In acute infections, glycolysis is the main energy source for the pro-inflammatory response and immune system activation [77, 102]. To promote an efficient and rapid response, membrane glucose transporters – Glut1, Glut3 and Glut4 – are overexpressed, with increased glucose uptake, dependent on

the PI3K/AKT (phosphatidylinositol-3-kinase/protein kinase B (also known as AKT)) and mammalian target of rapamycin (mTOR) signalling pathways [77, 129, 130]. The PI3K/AKT pathway is associated with cellular growth, survival, proliferation, and metabolism [131, 132]. This pathway is regulated by numerous upstream signalling proteins and regulates the activity of many effector proteins and pathways, among which are the hypoxia-inducible factor (HIF)-1α, and the mTOR pathway [131, 132]. The mTOR signalling pathway is associated with the identification of high nutrient availability and promotes cell growth and proliferation, being responsible for regulating autophagy, glucose uptake, glycolysis, oxidative phosphorylation, cholesterol, and fatty acid biosynthesis [131-133]. Furthermore, PI3K/AKT and mTOR signalling pathways regulate HIF-1α levels, which modulates the cell's metabolism and functions to ensure the cell's survival under hypoxia conditions [84, 131, 134]. Thus, under hypoxia conditions, as those associated with skin granulomas of acute *Leishmania* infections, high HIF-1α levels increase the activity of glycolysis followed by lactic fermentation, since it does not require oxygen to produce ATP [84, 131, 134].

Additionally, during the initial pro-inflammatory response of macrophages, almost all genes encoding host glycolytic enzymes are overexpressed, as well as enzymatic genes that control the rate of glycolysis, and enzymes that restore glucose levels through other pathways [99, 135, 136]. The presence of parasites drives macrophages into a Warburg-like response, with increased anaerobic glycolysis to resolve the infection more quickly [135]. This enhanced the M1 phenotype, facilitating an increased nucleotide flux through the PPP, with concomitant NADPH regeneration and consequently increased NO and ROS production [77, 102]. Also, M1-like macrophages have a slow and partially blocked TCA cycle, with consequent accumulation of citrate and succinate, which are engaged in mitochondrial ROS production [77, 102, 135]. Previous studies have shown that, in the early stages of infection, *Leishmania spp.* also actively induce macrophage Warburg-like aerobic glycolysis, as a host defence mechanism to resolve the infection [51, 102, 135]. However, after the first 18 hours of infection, intracellular *Leishmania* parasites induce a host metabolic switch from anaerobic glycolysis to increased mitochondrial oxidative phosphorylation, through the SIRT1-LKB1-AMPK (sirtuin 1 – liver kinase B1 – AMP-activated protein kinase) energetic signalling pathway [129]. This energetic signalling pathway is normally activated by a high intracellular AMP/ATP ratio, indicative of low energetic conditions, and induces catabolic processes to restore intracellular energy and nutrients [137]. *Leishmania* parasites take advantage of these processes and promote their persistence and proliferation [129].

Previous work from our group demonstrated that the inhibition of host glycolysis *in vitro* retracted important macrophage and neutrophils functions, that are crucial for controlling the infection [129, 138].

Also, the *in vivo* inhibition prior to *Leishmania* infection resulted in increased host susceptibility and increased parasite burden 7 days post-infection [138]. However, to our knowledge, no studies address glycolysis enhancement in the VL infection context. Furthermore, it is still unclear if it is possible to modulate glycolysis as an anti-leishmanial therapy. Thus, this master thesis project aimed to fill these gaps by addressing the glycolysis enhancement in the VL acute infection context and also consider the induced glycolytic increase as a potential adjuvant to the clinically applied anti-leishmanial therapies, in particular miltefosine, which is the only drug orally available [139].

RESEARCH OBJECTIVES

This master thesis project, driven by the hypotheses that **(1)** enhanced glycolysis may promote parasite clearance and that **(2)** enhanced glycolysis may improve the currently applied anti-*Leishmania* miltefosine efficacy, had two main objectives:

1. **The identification of the most effective drug in reducing the acute parasite load, by boosting host macrophage's glycolysis.** For this, we aimed to perform a drug screening of potential drugs in macrophages *in vitro* cultures.
    a. 1st stage – Identification of the drugs that reduced the parasite load, without compromising host cell viability.
    b. 2nd stage – Titration of the best 1st stage drug(s), to find the minimum effective dose.
    c. 3rd stage – Test the 2nd stage drug(s)' effect on host immune cells activation, pro-inflammatory response, glycolytic pathway, and parasite clearance.
    d. 4th stage – Clarify if the predicted drug-induced parasite clearance is through the host cell immune system response, with its glycolytic-promoted pro-inflammatory profile, and/or by direct parasite toxicity.
2. **Understand the *in vivo* impact of enhanced glycolysis as an adjuvant to the currently applied anti-*Leishmania* miltefosine efficacy in acute infection.** Within this, we intended to:
    a. Assess the importance of glycolysis enhancement in the acute phase of infection and the consequent development of the intracellular parasite load
    b. Address the possibility of enhanced glycolysis as an adjuvant to miltefosine and its combined effect on intracellular parasite clearance and possible disease resolution.

MATERIALS AND METHODS

M.1. Mice and Ethics Statement

The initial BALB/cByJ mice breeding pairs were purchased from Charles River Laboratories. Mice were maintained in accredited animal facilities at Life and Health Sciences Research Institute (ICVS), under standard conditions of 12h light/dark cycle, with a controlled temperature of 22°C, 55% of relative humidity and standard diet and water *ad libitum*. Both males and females with 8-16 weeks were used. Mice were euthanised by carbon dioxide (CO_2) inhalation, followed by cervical dislocation to confirm death.

The experiments followed the European Union Directive 2010/63/EU guidelines through the Portuguese Decree-Law 113/2013 of August 7th, terrified by Decree-Law 1/2019, and were conducted under the Portuguese national authority for animal experimentation – Direção Geral de Alimentação e Veterinária (DGAV) – guidelines on animal care and experimentation, with the approval of the local ethic committee – Organ Responsible for Animal Welfare of the School of Medicine and its Life and Health Sciences Research Institute and of the Institute 3Bs, University of Minho (ORBEA EM/ICVS-13Bs/3Bs) – under the SECVS 074/2016 process. The procedures were carried out by trained researchers with personal accreditation for laboratory animal manipulation and research.

M.2. Primary Murine Bone Marrow-Derived Macrophages

Femur and tibia of hind legs were removed in sterile conditions and rinsed in ethanol 70% v/v. The bones were cut at both extremities and bone marrow was flushed with sterile Dulbecco's Modified Eagle Medium (DMEM, ref. 10938-025 from Gibco™, ThermoFisher Scientific) supplemented with 10% v/v heat-inactivated Foetal Bovine Serum (FBS, ref. 10270-106, Gibco™), 1% v/v Penicillin-Streptomycin (Pen/Strep, 10.000 U/mL Pen, 10.000 µg/mL Strep, ref. 15140-122, Gibco™), 2 mM L-glutamine (ref. 25030-024, Gibco™), and 1% v/v 4-(2-hydroxyethyl)-1-piperazineethanesulfonic acid (HEPES) buffer 1M (ref. 15630-056, Gibco™). Viable HSCs, present in the flushed bone marrow, were counted in a Neubauer Chamber (ref. 0640030, Marienfeld Superior) and plated in sterile culture plates (ref. 30024 (24-well) and 30096 (96-well), SPL Life Sciences) at a density of 5×10^5/mL in complete DMEM (cDMEM, supplemented) medium. These cells were differentiated into bone marrow-derived macrophages (BMDMs) using 20 ng/mL of recombinant macrophage colony-stimulating factor (M-CSF, ref. 315-02-200UG, PeproTech®) and incubated at 37 °C with 5% CO_2 in a Heaeus HeraCell 150 incubator for 7 days. On the 4th day of differentiation, a second dose of 20 ng/mL of M-CSF supplementation was added to the medium. BMDMs were used with 7 days of differentiation.

M.3. Axenic *L. donovani* cultures

M.3.a. *L. donovani* culture maintenance

Cloned lines of virulent *L. donovani* (MHOM/IN/82/Patna1) were maintained with weekly sub-passages in Roswell Park Memorial Institute (RPMI) 1640 medium (ref. 21870-025, Gibco™), supplemented with 10% v/v heat-inactivated FBS, 100 U/mL & 100 mg/mL Pen/Strep, 2 mM L-glutamine, and 1% v/v HEPES buffer 1M (complete RPMI (cRPMI) medium), at 26°C in an orbital shaker-incubator ES-20/60 from Biosan. The axenic *L. donovani* cultures were maintained until their 10th sub-passage, upon which promastigotes lose their infectivity properties [140].

M.3.b. *L. donovani* toxicity assay

On day 0, *L. donovani* promastigotes at the same sub-passage were cultured in T25 flasks without filter (ref. 70125, SPL Life Sciences) at a density of 1×10^6 promastigotes/mL in cRPMI medium. Each *L. donovani* culture was cultured with a dose range of 0.1 to 50 µM of treatment compound, with one culture left untreated as control. The cultures were maintained at 26°C, and the promastigotes were daily counted for 9 days in a Neubauer chamber, while fixed with 2% paraformaldehyde (PFA, ref. 141451.1211, PanReac AppliChem, ITW Reagents).

M.4. *In vitro* infection and treatments

BMDMs with 7 days of differentiation were infected with stationary-stage *L. donovani* promastigotes (with 7 days of axenic growth) resuspended in fresh cRPMI medium, and incubated at 37°C, with 5% CO_2. After 4 hours of infection, the *L. donovani* suspension was removed and cells were washed 3 times with phosphate buffer saline (PBS, pH 7.4) to remove non-internalized promastigotes. Infected BMDMs were then incubated in cRPMI at 37°C, with 5% CO_2.

The *in vitro* treatments were performed with the doses and timepoints described in the respective experimental designs (Results section).

M.5. *In vivo* infection, treatments, and necropsy

BALB/cByJ male and female mice with 12-14 weeks old were infected with 1×10^8 virulent stationary-stage *L. donovani* promastigotes through a single intraperitoneal injection. *L. donovani* parasites were previously washed 2 times with apyrogenic PBS 1X, pH 7.4 (PBS 10X pH 7.4 ref. 70011-044, Gibco™, diluted in UltraPure™ Distilled Water ref. 10977-035, Invitrogen, Thermo Fisher Scientific) and resuspended in the same medium to a final concentration of 1×10^8 parasites per 100 µL. Between the

3rd and 7th days of infection, mice were treated with daily oral gavages (*per os*) of 20 mg/kg/day of meclizine, 20 mg/kg/day of miltefosine, the combination of both (daily successive *per os* administrations) or treated with 50% v/v DMSO in apyrogenic PBS as meclizine's vehicle control group. The DMSO dose applied to the control group was previously proven to be safe for mice [141]. Thus, 20 mg/kg/day was the selected meclizine dose to promote the highest parasite load elimination without exceeding 50% v/v of DMSO. Mice were closely monitored for any signs of distress and their welfare was preserved during the experiment. On the 10th day of *in vivo* infection, mice were euthanized by CO_2 inhalation, followed by cervical dislocation to confirm death, and spleen, liver, bone marrow, and colon were retrieved.

Spleen was dissociated through gentle compression against a sterile 70 µm nylon cell strainer (ref. 352350, Falcon®, Corning) with a plunger and washed with cRPMI medium to a 15 mL conical tube (ref. 51015, SPL Life Sciences). Splenocytes were centrifuged in a Heraeus Megafuge 1.0R centrifuge (Thermo® Electron Corporation) at 1 500 rpm for 5 min, resuspended in 10 mL of cRPMI and counted in a Neubauer chamber. A total of 1×10^7 splenocytes were resuspended in 1 mL of phenol:chloroform:isoamyl alcohol (P:C:I) 25:24:1 v/v, pH 8.0 (ref. P2069-400ML, Sigma-Aldrich®) for further deoxyribonucleic acid (DNA) extraction. Also, a total of 5×10^5 viable splenocytes per well were seeded in cRPMI in 96-well U-type plates (ref. 34096, SPL Life Sciences) for further flow cytometry analysis.

Mice liver and colon were stored at -80°C, and later a portion of them was homogenised in P:C:I with manual physical maceration in a Potter-Elvehjem tissue grinder homogenizer for further DNA extraction.

Finally, the bone marrow of one femur per mouse was flushed with cRPMI medium, centrifuged, and resuspended in 1 mL of P:C:I, for further DNA extraction.

M.6. Parasite Rescue and Transformation Assay

On the 4th day post-infection of the *in vitro* experiments, *L. donovani* viability was assessed by adapting the Parasite Rescue and Transformation Assay (PRTA) described in [142]. Briefly, the culture media was renewed, and the plates were sealed and incubated at 26°C to allow the conversion of amastigotes into promastigotes. After 7 days of incubation, the promastigotes were fixed by the addition of 50 µL of 2% PFA per 96-well (with 100 µL cRPMI) and further counted in a Neubauer Chamber with a 40x amplification objective.

M.7. Sulforhodamine B Assay

Host cell viability after *in vitro* infection was assessed through an adaptation of the sulforhodamine B (SRB) array described in [143]. BMDMs infected with *L. donovani*, maintained in sterile 96-well culture plates with 100 µL of cRPMI medium, were treated with the selected compounds and incubated at 37°C with 5% CO_2. On the 4th day post-infection, cells were fixed by the addition of 50 µL of previously refrigerated 50% trichloroacetic acid (ref. 131067.1611, PanReac) to each well and incubated at 4°C for 60 min. The plates were then rinsed with deionized water and allowed to dry at room temperature. After complete drying, cellular proteins were stained with 100 µL of 0,4% SRB (ref. S9012-5G, Sigma-Aldrich®) in 1% acetic acid glacial (ref. 401424, CARLO ERBA Reagents) for 30 min at room temperature. The excess SRB was removed by successive washes with 1% acetic acid and the plates were allowed to dry at room temperature. The SRB complexed with cellular proteins was solubilized in 100 µL of 10 mM Tris buffer (ref. 648313, Calbiochem), and the absorbance was measured at 515 nm in an Infinite® M200 NanoQuant plate reader (from TECAN).

M.8. High-Performance Liquid Chromatography

Extracellular glucose and lactate concentrations were quantified in the *in vitro* conditions' supernatant by high-performance liquid chromatography (HPLC). A HyperREZ™ XP Carbohydrate H^+ HPLC Column (ref. 69008-307780, ThermoFisher® Scientific) was installed in the HPLC system and equilibrated at 54°C with a flow rate of 0.7 mL/min of mobile phase. The mobile phase used was 2.5 mM sulfuric acid (ref. 131058.1212, PanReac) in ultrapure water (Milli-Q® IQ 7005 Pure and Ultrapure Water Purification System), previously filtered (0.22 µm polyethersulfone filter, ref. 431097, Corning®) and degassed for at least 45 min. The samples were centrifuged in a Heraeus Megafuge 1.0R centrifuge at 1 500 rpm for 5 min to remove debris and loaded into the HPLC autosampler (234 autoinjector from Gilson®). The samples were carried, one by one, by the mobile phase through the column (stationary phase) at a 0.7 mL/min flow rate and were detected by a Gilson® refractive index detector IOTA 2, with sensitivity set at 8. Glucose and lactate were detected with retention times of 7-9 min and 11-13 min, respectively, and the area under the curve for each of them was acquired and analysed in the Gilson® UniPoint Software (version 5.11). Areas under the curve were then converted into concentrations of the respective carbohydrate with established standard lines.

M.9. Flow Cytometry

The host immune cells' phenotypical characterization was performed by flow cytometry. In the *in vitro* experiments, BMDMs seeded in 24-well plates were detached in incomplete RPMI medium using a cell scrapper (ref. 90020, SPL Life Sciences) and transferred to a 96-well U-type plate. The medium was retrieved, and cells were stained with anti-mouse monoclonal antibodies according to the antibody panel described in **Table 1**. After incubation at 4°C for 15 min, cells were rinsed with FACS buffer (2% FBS in PBS), fixed for 10 min with 2% PFA, and resuspended in FACS buffer. Samples were acquired on a LSR II flow cytometer (BD Biosciences), and data was analysed using FlowJo software (version 10, TreeStar).

Table 1. Flow cytometry antibody panel applied in the *in vitro* experiments

Target Antigen	Monoclonal Antibody		
	Clone	Fluorochrome	Supplier
I-A/I-E (MHC class II)	M5/114.15.2	BV605	Biolegend®
CD86	GL-1	APC-Cy7	Biolegend®
CD206	C068C2	FITC	Biolegend®
CD301	LOM-14	PE	Biolegend®

In the same manner, mice splenocytes, retrieved from the *in vivo* infection and seeded in 96-well plates U-type, were stained with anti-mouse monoclonal antibodies for their surface markers antigens, according to the antibody panels described in **Table 2**. Stained splenocytes were rinsed with FACS buffer, fixed with 2% PFA, and resuspended in FACS buffer. Samples were acquired on a LSR II flow cytometer, and data was analysed using FlowJo software.

Table 2. Flow cytometry antibody panels applied in the *in vivo* experiment

Target Antigen	Monoclonal Antibody		
	Clone	Fluorochrome	Supplier
CD3	145-2C11	BV510 (Amcyan)	Biolegend®
CD4	REA604	APC-Cy7	Miltenyi
CD8	53-6.7	BV711	Biolegend®
CD44	IM7	PerCP-Cy5.5	Biolegend®
CD62L	MEL-14	BV605	Biolegend®

M.10. Enzyme-Linked Immunosorbent Assay

The cytokines levels were quantified in the *in vitro* conditions' supernatant by enzyme-linked immunosorbent assays (ELISA). Following the manufacturer's instructions, the mouse TNF-α (ref. 88-7324-88, Invitrogen), mouse IL-6 (ref. 88-7064-88, Invitrogen), and mouse IL-10 (ref. 88-7105-88, Invitrogen) uncoated ELISA kits were applied.

M.11. RNA extraction and complementary DNA synthesis

Total RNA was isolated from infected and non-infected BMDMs using Trizol (TripleXtractor, ref. GB23, GRiSP®), according to the manufacturer's instructions. The RNA concentration and purity were measured using a NanoDrop® 1000 Spectrophotometer (Thermo Fisher Scientific) and 250 ng of total RNA was reverse transcribed using the Xpert cDNA Synthesis Mastermix Kit (ref. GK81.0100, GRiSP®), following the manufacturer's instructions.

M.12. DNA extraction

In the *in vivo* experiment, the total DNA was extracted from the spleen, liver, bone marrow and colon of infected mice. Cells from these organs, previously resuspended in P:C:I, were centrifuged in a refrigerated Centurion Scientific Pro Analytical C2000R centrifuge at 13 000 rpm for 10 min at 4°C. The upper aqueous phase, where the DNA is located, was carefully removed and transferred to a new DNAse/RNAse-free 1.5 mL microcentrifuge tube (ref. 72.691, SARSTEDT). The aqueous phase volume was measured, an equal volume of sodium acetate 3M (ref. 131633, Panreac) was added, as well as 20 µg of glycogen (ref. 10901393001, Roche), and 2.5 times the volume of aqueous phase plus sodium acetate of 100% ethanol (ref. 4146052, Carlo Erba Reagents). The samples were stored at -20°C overnight to precipitate the DNA.

On the following day, samples were centrifuged at 13 000 rpm for 30 min at 4°C, and the supernatant was carefully removed without disturbing the DNA pellet. Samples were rinsed twice with 70% ethanol and centrifugations of 13 000 rpm for 5 min at 4°C to remove any residual from previous solvents. Samples' DNA pellet was left to dry at room temperature and resuspended in 50 µL of UltraPure™ Distilled Water. The DNA concentration and purity were measured using a NanoDrop® 1000 Spectrophotometer, and the samples' DNA was stored at -20°C until further analysis.

M.13. Real-time quantitative polymerase chain reaction

Real-time quantitative polymerase chain reactions (qPCR) were run for each sample on an Applied Biosystems® 7500 Fast Real-Time PCR system (Life Technologies™). In the *in vitro* experiments, target gene sequences, present in the complementary DNA obtained from extracted RNA, were selected and amplified using the primers presented in **Table 3** and the NZY Speedy qPCR Green Master Mix (ref. MB224, NZYTech®). In the *in vivo* experiment, *L. donovani* burden was assessed through *L. donovani* kinetoplastid DNA (primers sequence in **Table 3**) quantifications in samples' total DNA using a TaqMan-based qPCR assay [134].

After amplification, the amplification curves were analysed using the Design & Analysis Software (version 2.6.0, Applied Biosystems®) and the retrieved cycles of quantification values (Cq values) were normalized to the expression of the housekeeping gene 18S. Gene expression changes were calculated using the log transformation of the $2^{-\Delta\Delta C_q}$ method [144].

Table 3. Primers used in the qPCR reactions and respective nucleotide sequences

Genes		Forward Primer Sequence	Reverse Primer Sequence	Supplier
Housekeeping	18S	5'-GTAACCCGTTGAACCCCATT-3'	5'-CCATCCAATCGGTAGTAGCG-3'	Alfagene®
Targets (*in vitro*)	TNF-a	5'-GCCACCACGCTCTTCTGTCT-3'	5'-TGAGGGTCTGGGCCATAGAAC-3'	IDT™
	IL-6	5'-ACACATGTTCTCTGGGAAATCGT-3'	5'-AAGGCATCATCGTTGTTCATACA-3'	IDT™
	IL-10	5'-GCTCCACTGCCTTGCTCTTATT-3'	5'-AGGACTTTAAGGGTTGGGTT-3'	IDT™
	H1R	5'-GTGTGAGGGGAACAGGACAG-3'	5'-TACAGCACCAGCAGGTTGAG-3'	IDT™
	PFKFB3	5'-TGTCCAGCAGAGGCAAGAAG-3'	5'-TCTCGTTGAGTGCCTTCCAC-3'	IDT™
	PCYT2	5'-AGGCTGGGAGGTACAGAGAG-3'	5'-ATCTCCTGGCTGCTGTGATG-3'	IDT™
Target (*in vivo*)	*Leishmania kinetoplastid DNA*	5'-CTTTTCTGGTCCTCCGGGTAGG-3'	5'-CCACCCGGCCCTATTTTACACCAA-3'	Invitrogen

M.14. Statistical Analysis

Statistical analyses were performed with GraphPad Prism 8.4.2. software. Outliers were identified and removed using the ROUT method, with Q = 5%. The normality of samples was assessed with the Shapiro-Wilk test. Accordingly with the respective experimental data, samples were analysed with a one-way ANOVA with Bonferroni post-hoc test, a Friedman test followed by Dunn's post hoc correction, or in samples with missing values, with a Kruskal-Wallis test followed by Dunn's post hoc correction. When adequate, a Spearman's Rank-Order Correlation test was also applied. The statistical details of each experiment can be found in figure legends and data are presented as mean with standard deviation in

data analysed with parametric tests, and as median with interquartile range in data analysed with non-parametric tests. Statistically significant p values are represented as follows: *p < 0.05, **p <0.01, ***p <0.001.

RESULTS

R.1. Drug Screening

Driven by the hypothesis that enhanced glycolysis may promote parasite clearance, we aimed for the identification of the most effective drug in reducing the acute parasite load, by boosting host macrophage's glycolysis, without compromising host cell viability. To this end, we used an *in vitro* model where mice BMDMs were infected with virulent *L. donovani* promastigotes and treated at 7 hours post-infection or at 2 days post-infection with compounds that were able to induce the host glycolysis (and consequent conversion of pyruvate to lactate), with a preference for those already clinically available or in clinical trials. Considering the respective mechanism of action in the glycolytic pathway, we selected **(1)** inhibitors of HIFs prolyl 4-hydroxylases – Daprodustat (ref. 19915-1MG, Cayman Chemical), Dimethyloxalylglycine (DMOG, ref. 400091-50MG, Sigma-Aldrich®), FG-2216 (ref. 18382-1MG, Cayman Chemical) and Roxadustat (ref. 15294-5MG, Cayman Chemical) – that stabilize increased HIFs levels (such as HIF-1α levels) [130]; **(2)** enhancers of the phosphoglycerate kinase 1 (PGK1) activity – Alfuzosin (ref. 13648-5MG, Cayman Chemical) and Terazosin (ref. PHR1721-1G, Sigma-Aldrich®) [145]; and **(3)** Meclizine, that activates the phosphofructokinase (PFK) through increased levels of 6-phosphofructo-2-kinase/fructose-2,6-biphosphatase 3 (PFKFB3) [146, 147] (**Figure 3**).

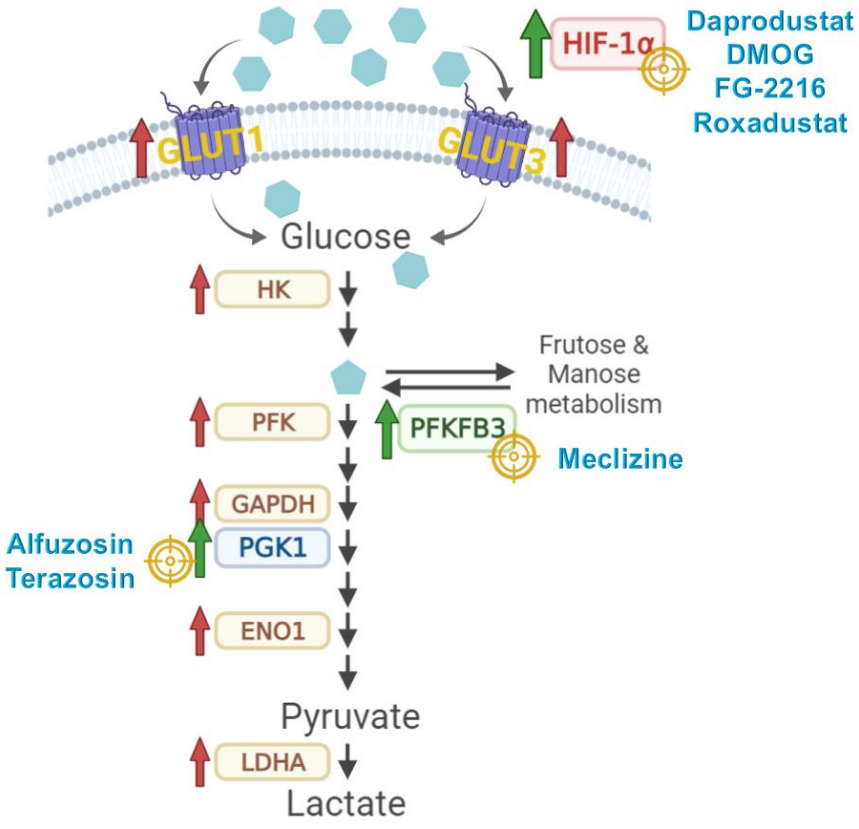

Figure 3. Glycolytic targets of the tested compounds. Daprodustat, Dimethyloxalylglycine (DMOG), FG-2216 and Roxadustat are inhibitors of hypoxia-inducible factors (HIFs) prolyl 4-hydroxylases, which stabilize increased HIF-1α levels. This leads to the increase of glucose transporters Glut1 and Glut3 expression, as well as the increase of expression and activity of the glycolytic enzymes hexokinase (HK), glyceraldehyde-3-phosphate dehydrogenase (GAPDH), enolase 1 (ENO1) and the fermentative enzyme lactate dehydrogenase A (LDHA) (marked with red arrows). Alfuzosin and Terazosin enhance the phosphoglycerate kinase 1 (PGK1) activity. Meclizine increases the levels of 6-phosphofructo-2-kinase/fructose-2,6-biphosphatase 3 (PFKFB3), with consequent enhancement of the phosphofructokinase (PFK) activity. Schematic representation created with BioRender.

Accordingly, infected BMDMs were treated with 100 nM, 1 μM, or 10 μM of each compound at 7h post-infection or at 2 days post-infection, with 10 μM of Miltefosine (ref. M5571-50MG, Sigma-Aldrich®) as a positive control for parasite clearance in each timepoint. The medium was renewed when the treatments were applied, and the cells were kept in contact with the latter until the 4th day post-infection, when we assessed the parasite load, macrophage viability, and glucose and lactate concentrations. The experimental design is represented in **Figure 4**.

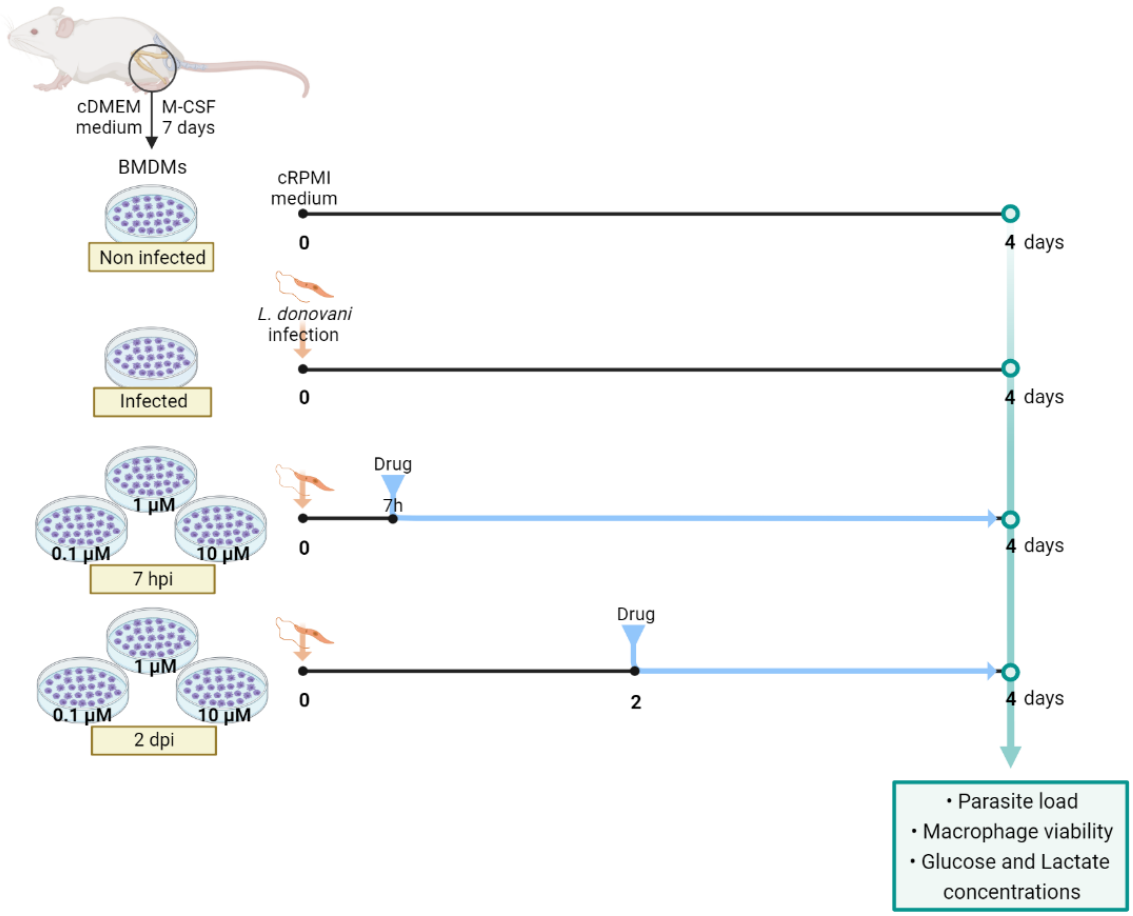

Figure 4. Drug screening test *in vitro*. Primary BALB/cByJ bone marrow-derived macrophages (BMDMs, 5×10^5/mL), previously differentiated from bone-marrow hematopoietic stem cells (HSCs) in contact with macrophage colony-stimulating

factor (M-CSF) for 7 days, were infected with virulent stationary-stage *L. donovani* promastigotes (MHOM/IN/82/Patna1) (10:1 promastigotes/BMDMs ratio) and treated at 7h post-infection or at 2 days post-infection with a glycolysis-inducing drug, with 10 μM of miltefosine as parasite clearance positive control. A dose of 100 nM, 1 μM and 10 μM of each selected drug was administered. On the 4th day post-infection, the parasite load was assessed through and adaptation of the parasite rescue and transformation assay (PRTA) [142], the macrophage viability was assessed through the sulforhodamine B assay, and extracellular glucose and lactate concentrations were quantified in the supernatant by high-performance liquid chromatography (HPLC). Schematic representation created with BioRender.

We observed that, among the different compounds tested, meclizine presented the most parasite burden reduction, with apparent increased effectiveness when applied at 2 days post-infection (**Figure 5**), without compromising host cell viability (**Supplementary Figure 1**). This meclizine-induced reduction of the parasite load was shown to be dose-dependent in a statistically significant manner, with a Spearman's Rank-Order Correlation r (r_s) of $r_s(16) = -0.553$, 95% confidence interval (CI) of -0.816 to -0.102, $p = 0.017$, and may also be time-dependent, despite not being statistically significant ($r_s(16) = -0.417$, 95% CI of -0.747 to 0.076, $p = 0.085$). However, the application of this treatment, in both timepoints, does not seem to induce any alteration in the lactate/glucose ratio, a calculated ratio between the lactate secretion and glucose consumption by cells (**Figure 6.A** and **Figure 6.B**). This ratio can be used as an indicator of the cell's metabolic preference for lactic fermentation after glycolysis (ratio close to 2 mol/mol), or for other metabolic pathways such as oxidative phosphorylation (energy production) or PPP (nucleotides and NADPH synthesis), presenting lower lactate/glucose ratios.

Among the other treatments tested, daprodustat, DMOG, FG-2216 and roxadustat induced a notable increase in the parasite load (**Figure 5**), and alfuzosin and terazosin, even after experimental replications (data not shown), did not demonstrate a clear dose-dependent effect on the parasite load, so they were excluded from the following experiments. Also, only daprodustat, DMOG and Roxadustat demonstrate an apparent effect on the lactate/glucose ratio with the applied doses (**Figure 6**).

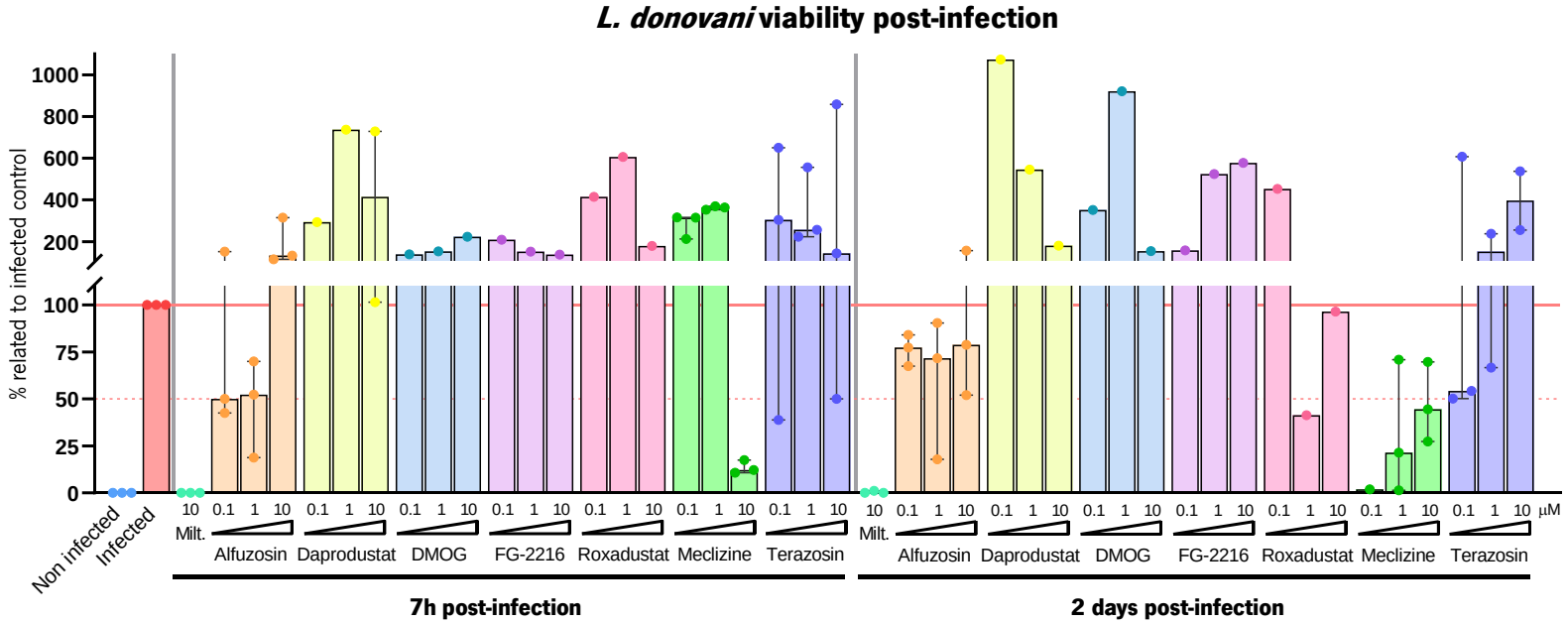

Figure 5. Meclizine presents the highest induced parasite load reduction *in vitro*. The parasite load was analysed after 4th day post-infection through the PRTA and the number of viable *L. donovani* parasites in infected BMDMs after treatment was normalized against the respective untreated control (infected). A correlation matrix was computed for meclizine data, with a statistically significant Spearman's Rank-Order Correlation r of $r_s(16) = -0.553$, 95% CI of -0.816 to -0.102, $p = 0.017$ between meclizine dose and the relative percentage of viable parasites, and a non-significant correlation of $r_s(16) = -0.417$, 95% CI of -0.747 to 0.076, $p = 0.085$ between the timepoint of treatment and the relative percentage of viable parasites. $1 \leq n \leq 3$ mice.

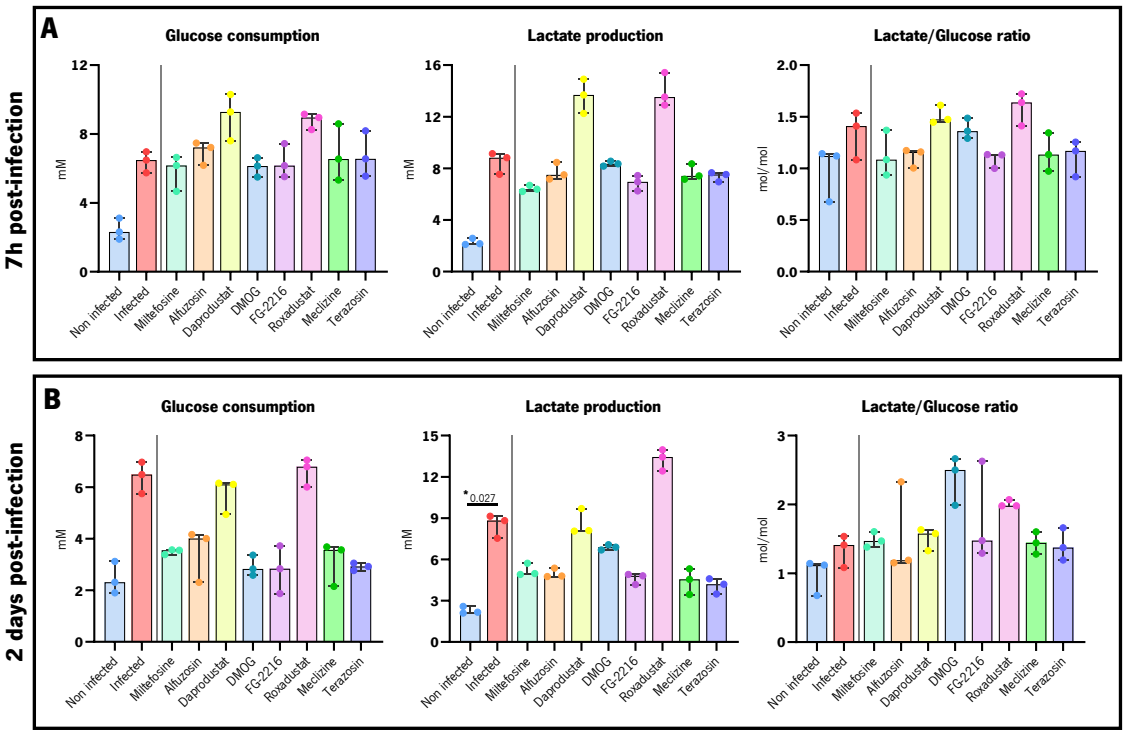

Figure 6. Only Daprodustat, DMOG and Roxadustat demonstrate an apparent effect on the lactate/glucose ratio. (A) and (B) Glucose consumption and lactate production were assessed on the 4th day post-infection through the respective extracellular concentration's quantifications by HPLC. The lactate/glucose ratio was calculated between the lactate secretion and glucose consumption of cells under each treatment and timepoint. Friedman's tests applied to each data set showed statistically significant differences between the applied treatments: *(A.1)* Glucose: $X^2(9) = 23.80$, $p = 0.005$; *(A.2)* Lactate: $X^2(9) = 25.11$, $p = 0.003$; *(A.3)* Lactate/Glucose ratio: $X^2(9) = 23.15$, $p = 0.006$; *(B.1)* Glucose: $X^2(9) = 20.09$, $p = 0.017$; *(B.2)* Lactate: $X^2(9) = 25.18$, $p = 0.003$; *(B.3)* Lactate/Glucose ratio: $X^2(9) = 17.55$, $p = 0.041$; n = 3 mice.

R.2. Meclizine dose-response of infected macrophages

Based on the drug screening data, we proceeded with an *in vitro* dose-response characterization of infected macrophages treated with meclizine after 2 days of infection. In this sense, mice BMDMs infected with *L. donovani* were treated at 2 days post-infection with a dose range of 0.1 to 50 µM of meclizine and on the 4th day post-infection we analysed the parasite load, macrophage viability and phenotype, glucose consumption and lactate production, and macrophages' cytokine secretion. The experimental design is represented on **Figure 7**.

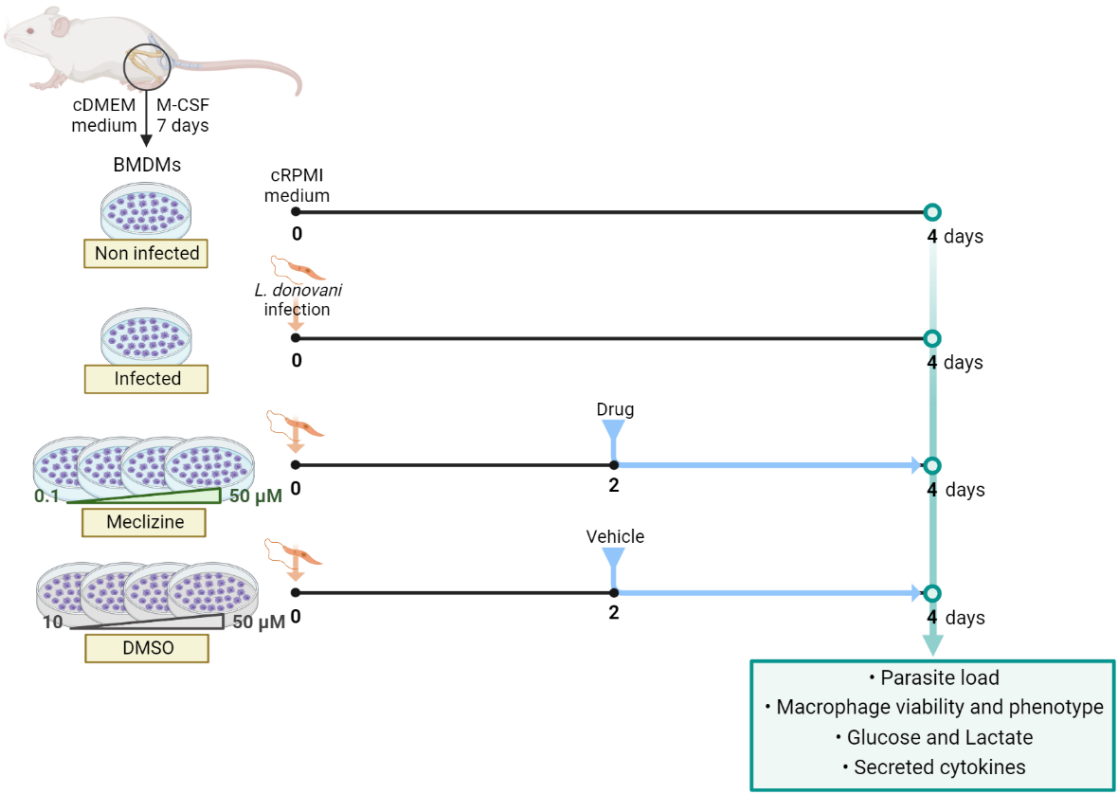

Figure 7. Dose-response of infected macrophages *in vitro*. Primary BALB/cByJ BMDMs (5×10^5/mL), with 7 days of differentiation with M-CSF, were infected with virulent stationary-stage *L. donovani* promastigotes (10:1 ratio) and treated at 2 days post-infection with a 0.1 – 50 µM dose range of meclizine, treated with meclizine's vehicle – dimethyl sulfoxide (DMSO) in a volume equivalent to 10 – 50 µM of meclizine, or left untreated as the negative control. On the 4th day post-infection, the parasite load was assessed through the PRTA, macrophage viability was assessed through the sulforhodamine B assay, macrophage phenotype and activation were assessed by flow cytometry, extracellular glucose and lactate concentrations were quantified by HPLC, and secreted cytokines were quantified by enzyme-linked immunosorbent assay (ELISA).

We observed a dose-dependent reduction of parasite burden in infected macrophages, with a meclizine half maximal inhibitory concentration (IC_{50}) of 13.15 µM, with a 95% CI of 7.31 to 25.66 µM (**Figure 8.A**). Also, this reduction in the parasite viability did not interfere with the viability of infected macrophages, which only suffered with higher doses of meclizine, such as 50 µM (infected BMDMs' mean viability of 52.42% ± 11,69%, p <0.001) (**Figure 8.B**).

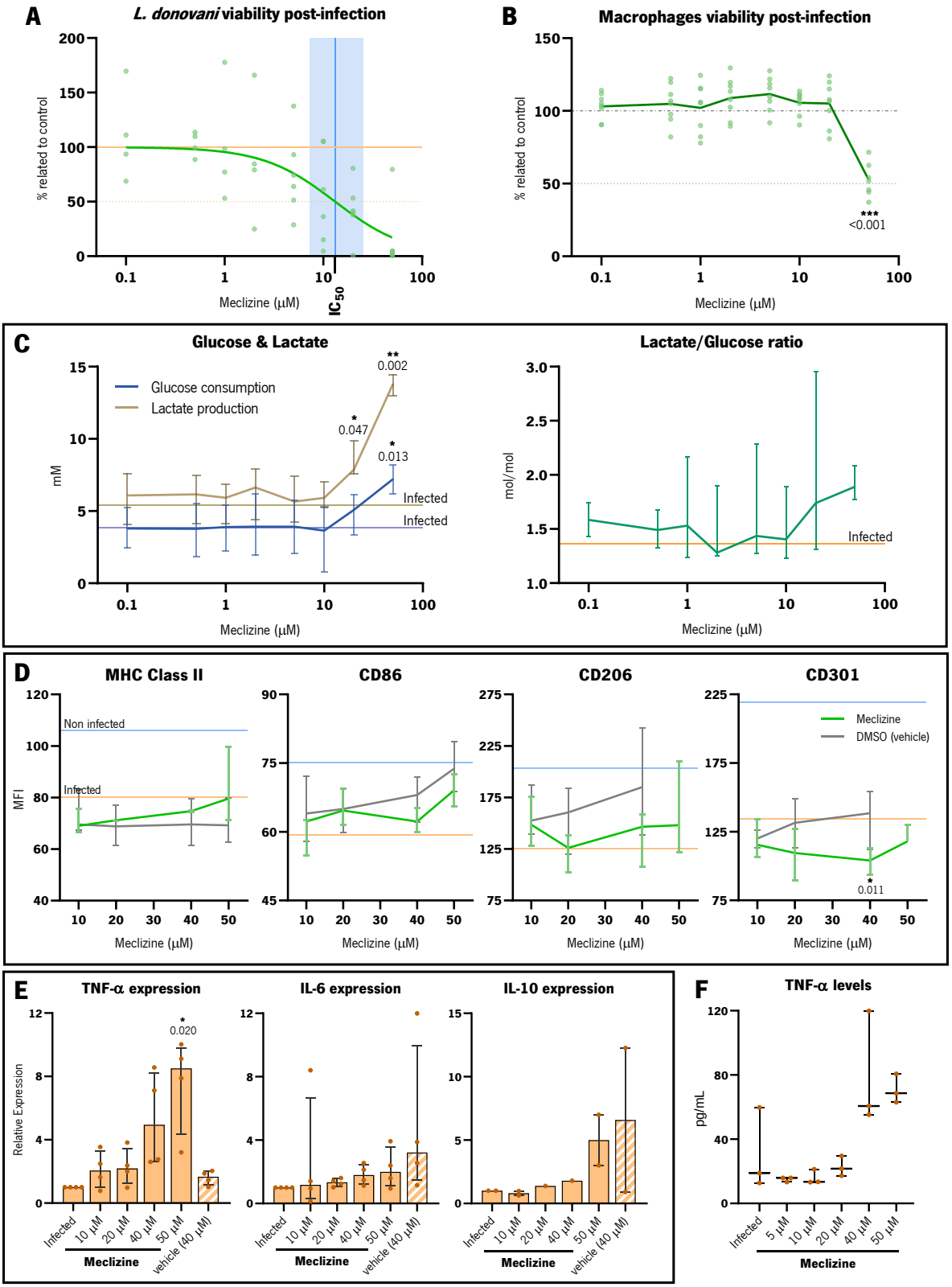

Figure 8. Meclizine induces a significant parasite burden reduction *in vitro* with doses close to 10 μM, but only promotes a macrophage M1-like polarization with 40 to 50 μM doses. (A) The parasite load was assessed through the PRTA and the number of viable *L. donovani* parasites in infected BMDMs after treatment was normalized against the respective untreated control. A sigmoidal curve was fitted to the experimental data, with an R^2 = 0.458, IC_{50} = 13.15, 95%

CI of 7.31 to 25.66. 4 ≤ n ≤ 6 mice, from two independent experiments. **(B)** The infected macrophage viability after treatment was assessed through the Sulforhodamine B assay and the measured absorbances were normalized against the respective untreated control. A one-way ANOVA, with Bonferroni post-hoc test revealed a statistically significant reduction in the macrophage viability when treated with 50 μM meclizine (52.42 ± 11.69 %, $p < 0.001$). 7 ≤ n ≤ 8 mice, from two independent experiments. **(C)** Glucose consumption and lactate production were assessed through the respective extracellular quantifications by HPLC. Friedman's tests applied to each data set showed statistically significant differences between applied doses. Glucose: $X^2(8) = 26.04$, $p = 0.001$; Lactate: $X^2(7) = 24.06$, $p = 0.001$. n = 6. The consequent lactate/glucose ratio was calculated, with no evident statistical differences through the applied Kruskal-Wallis H test $X^2(8) = 7.79$, $p = 0.454$. Data from two independent experiments. 4 ≤ n ≤ 6 mice, from two independent experiments. **(D)** The macrophage surface markers expression was assessed through flow cytometry and presented as the median fluorescence intensity (MFI) of the fluorochromes associated to the monoclonal antibodies against the target surface markers. Kruskal-Wallis H tests applied to each data set showed a statistically significant difference in the CD301 expression: $X^2(4) = 10.32$, $p = 0.035$; MHC class II: $X^2(4) = 5.16$, $p = 0.272$; CD86: $X^2(4) = 8.09$, $p = 0.088$; CD206: $X^2(4) = 4.31$, $p = 0.366$. 3 ≤ n ≤ 4 mice. **(E)** The infected macrophages TNF-α, IL-6 and IL-10 expression was assessed 6 hours after treatment through qPCR analysis. Data was normalized to the housekeeping 18S gene and compared between conditions using the $2^{-\Delta\Delta Cq}$ method. The applied Friedman's tests (TNF-α and IL-6) and Kruskal-Wallis H test (IL-10) showed a statistically significant difference in the TNF-α expression: $X^2(5) = 13.14$, $p = 0.022$; IL-6: $X^2(5) = 7.43$, $p = 0.191$; IL-10: $X^2(5) = 5.21$, $p = 0.467$. 1 ≤ n ≤ 4 mice. **(F)** The infected macrophages TNF-α extracellular levels were assessed through ELISA on the 4th day post-infection. Friedman's test applied showed a statistically significant difference between doses: $X^2(5) = 11.95$, $p = 0.008$. n = 3 mice.

Regarding glucose consumption and lactate production, we observed a gradual and statistically significant increase in both when treated with meclizine doses of 10 to 50 μM (**Figure 8.C**). Also, the consequent lactate/glucose ratio appears to increase slightly in the same dose range, which may indicate a progressive metabolic preference for lactic fermentation, although not statistically significant. However, considering that the viability of infected macrophages is affected with meclizine doses close to 50 μM, this apparent preference for lactic fermentation may be a combinatory result of cell death-associated mechanisms (at 50 μM) and a possible increase in the macrophage M1-like polarization between 10 μM and 50 μM of meclizine, which might be associated with the observed gradual increase in glucose consumption and lactate production in this dose range (**Figure 8.C**).

To clarify this question, we addressed, under the same *in vitro* conditions, the phenotype of *L. donovani*-infected macrophages and their cytokine secretion. By analysing the expression of the surface markers MHC class II, CD86, CD206 and CD301, it is possible to distinguish between macrophages with the M1-like pro-inflammatory phenotype and macrophages with the M2-like anti-inflammatory phenotype. MHC class II is constitutively expressed in APCs, being more prevalent in the pro-inflammatory macrophage phenotype [148]. In this manner, MHC class II and CD86 are classically associated with the

M1-like phenotype, and the CD206 and CD301 surface markers are associated with the M2-like phenotype [148-150]. In the tested dose range from 10 to 50 μM, we did not observe statistically significant differences in the expression of the surface markers MHC class II, CD86 or CD206, although the expression of the CD86 marker displays an apparent tendency to increase with increasing meclizine dose (**Figure 8.D**). On the other hand, we observed a significant reduction in the expression of the CD301 marker when infected macrophages are treated with 40 μM (**Figure 8.D**).

To shed light on the phenotype of the treated infected macrophages, we analysed the expression and extracellular levels of pro- and anti-inflammatory cytokines associated with the macrophage M1-like and M2-like phenotypes, respectively. In this manner, after 6 hours of treatment (on the 2nd day post-infection), we analysed by qPCR the expression of the pro-inflammatory cytokines TNF-α and IL-6, and the anti-inflammatory cytokine IL-10. We observed a statistically significant increase in the TNF-α transcription with 50 μM meclizine treatment (**Figure 8.E**). Furthermore, an increase in the extracellular TNF-α levels was observed on the 4th day post-infection, although this was not statistically significant (**Figure 8.F**). On the other hand, we did not observe any significant modifications in the transcript levels of IL-6 and IL-10 upon meclizine treatment on infected macrophages (**Figure 8.E**). Also, the extracellular levels of IL-6 and IL-10 were below the sensitivity of the respective ELISA kits. These data indicate an increase in the pro-inflammatory TNF-α, which is suggestive of an increase in the M1 macrophage polarization when treated with high doses of meclizine.

However, this apparent increase in the M1-like phenotype is only evident with doses of 40 to 50 μM of meclizine, while we observed a reduction in the parasite load already with doses close to 10 μM. This suggests that meclizine has a direct effect on the parasite at lower doses, to which is added a effect of meclizine on the host at higher doses.

R.3. Meclizine dose-response of axenic *L. donovani* cultures and non-infected macrophages

R.3.a. Axenic *L. donovani* cultures

To tackle meclizine's direct effect on *L. donovani* viability and/or proliferation, we cultured *L. donovani* axenic cultures with a dose range of 0.1 to 50 μM of meclizine (day 0) and counted daily the number of viable *L. donovani* promastigotes for the next 9 days in a Neubauer chamber. We observed an impaired growth of axenic promastigotes cultures when treated with higher doses of meclizine. Furthermore, the

axenic growth impairment showed to be dose-dependent on meclizine, with a Spearman correlation of $r_s(7) = -0.881$, $p = 0.007$ (**Figure 9**).

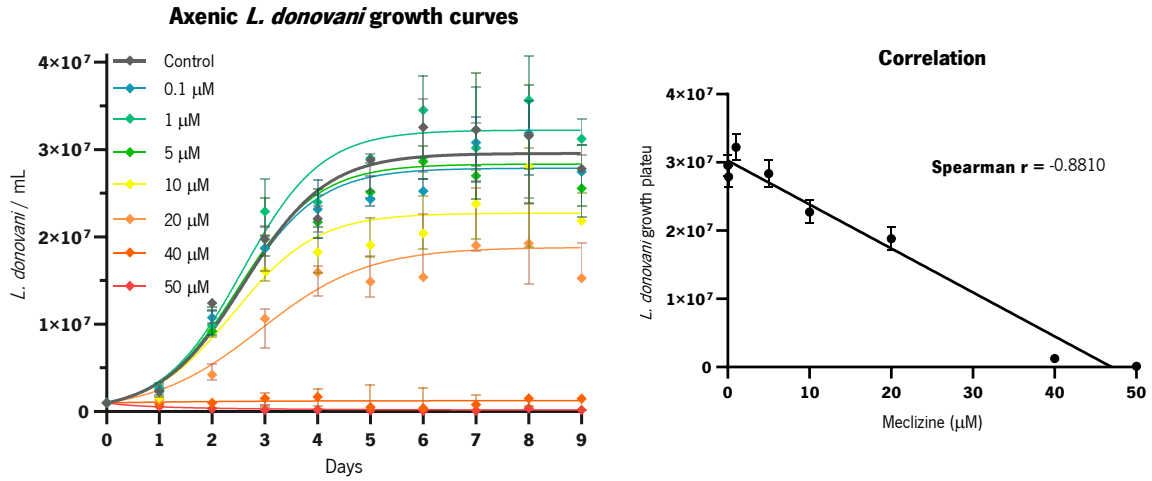

Figure 9. Meclizine induces a dose-dependent impairment in the growth of axenic cultures of *L. donovani* promastigotes. The viable parasites present in each of the treated axenic cultures were counted daily in a Neubauer chamber and data is presented as *L. donovani* / mL. Logarithmic curves were computed for each *L. donovani* axenic culture, with associated R^2 being higher than 0.900 for cultures treated with meclizine doses below or equal to 10 µM; $R^2 = 0.885$ for the culture treated with 20 µM; and failed to fit this model to cultures treated with 40 and 50 µM. n = 3 from independent experiments. The calculated medians for *L. donovani* concentration at each timepoint and dose were plotted against meclizine concentration and a Spearman's Rank-Order Correlation r was calculated ($r_s(7) = -0.881$, $p = 0.007$).

R.3.b. Meclizine dose-response of non-infected macrophages

To confirm if the effect of meclizine on the parasite load of infected macrophages is merely through direct parasite toxicity or whether it also has activity through the host macrophage metabolism and phenotype, we analysed the *in vitro* effect of meclizine on non-infected macrophages phenotype, according to the experimental design represented in **Figure 10**.

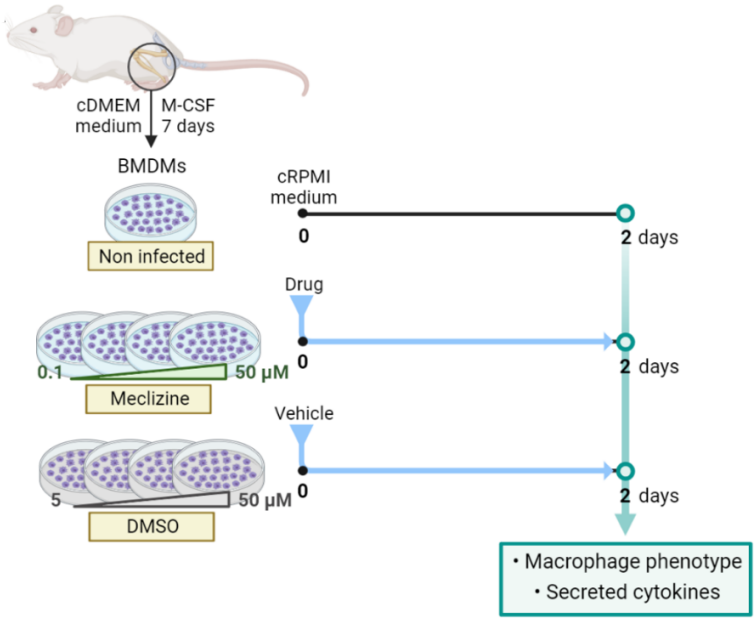

Figure 10. Dose-response of non-infected macrophages *in vitro*. Primary BALB/cByJ BMDMs (5×10^5/mL), with 7 days of differentiation with M-CSF, were treated with a 0.1 – 50 µM dose range of meclizine, treated with DMSO in a volume equivalent to 5 – 50 µM of meclizine, or left untreated as the negative control. On the 2nd day post-treatment, macrophage phenotype and activation were assessed by flow cytometry, and secreted cytokines were quantified by enzyme-linked immunosorbent assay (ELISA).

Similar to what is observed in infected macrophages (**Figure 8**), we observed a statistically significant increase in the CD86 expression and an apparent reduction in the expression of the CD301 marker (not statistically significant) in non-infected macrophages treated with higher meclizine doses (**Figure 11.A** vs. **8.D**). Also, there is a statistically significant increase in the TNF-α expression when cells are treated with 40 and 50 µM of meclizine (**Figure 11.B** vs. **8.E**). Conversely, there are no differences in the extracellular levels of TNF-α (**Figure 11.C** vs. **8.F**). Once more, the extracellular levels of IL-6 and IL-10 were below the detection limit of the respective ELISA kits.

In short, these data suggest a meclizine-induced macrophage polarization to the M1-like phenotype with 40 to 50 µM doses (**Figure 11.A** and **11.B**), which, alongside data from infected macrophages (**Figure 8.D** and **8.E**), is potentiated in the context of infection, with extracellular accumulation of TNF-α (**Figure 8.F**).

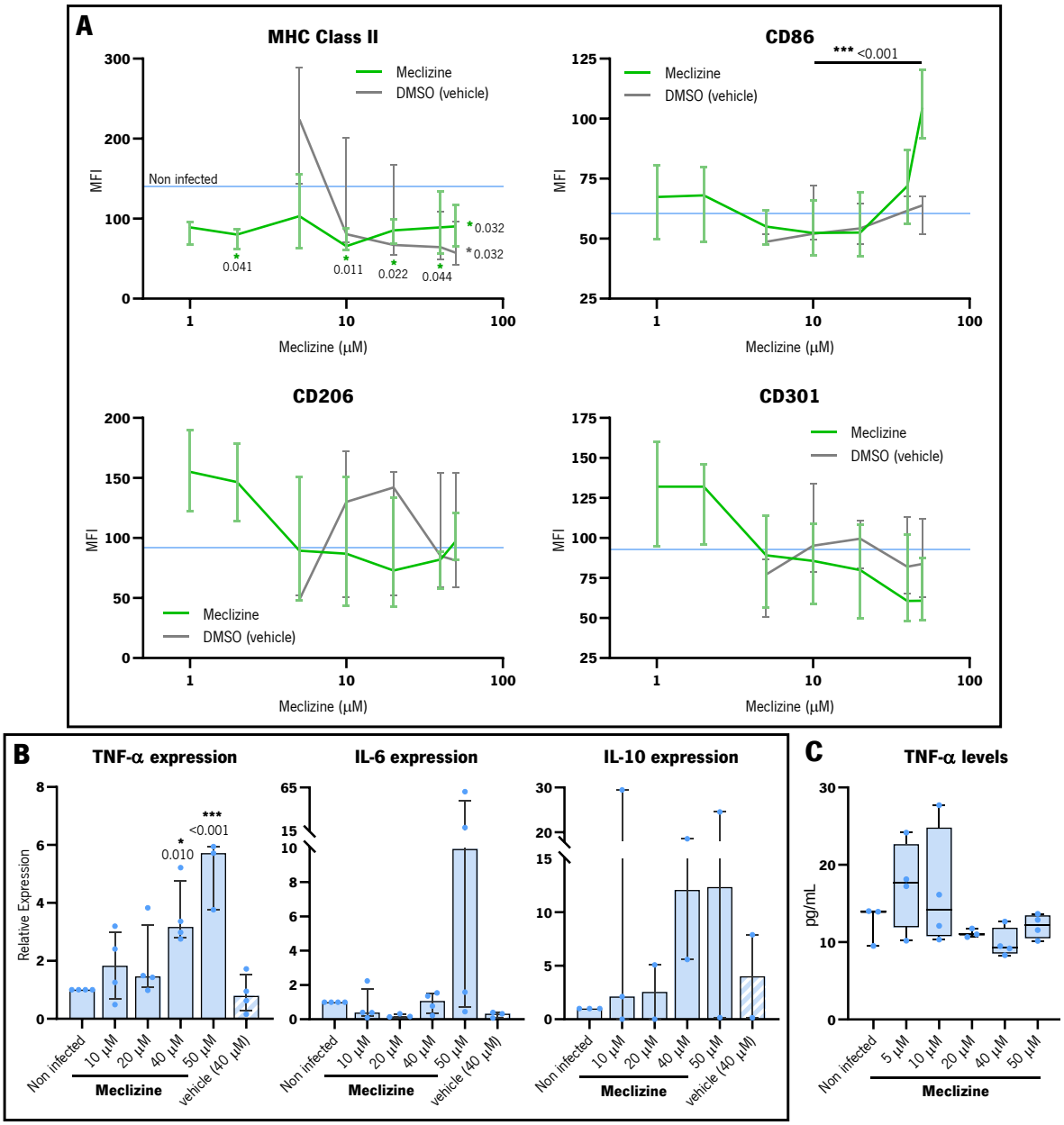

Figure 11. Meclizine induces a M1-like macrophage polarization in *in vitro* non-infected macrophages with 40 to 50 μM doses. (A) Non-infected BMDMs surface markers expression was assessed through flow cytometry and presented as MFI. The applied statistical analysis showed statistically significant differences in the MHC class II and CD86 expression between applied meclizine doses. Meclizine treatments: MHC class II – one-way ANOVA ($F(7, 45) = 2.58$, $p = 0.025$); CD86 – Friedman test ($X^2(5) = 27.77$, $p < 0.001$); CD206 – one-way ANOVA ($F(7, 48) = 2.03$, $p = 0.070$); CD301 – one-way ANOVA ($F(7, 48) = 2.67$, $p = 0.020$). Vehicle treatment in MHC class II – Kruskal-Wallis H test ($X^2(5) = 14.94$, $p = 0.011$). $4 \leq n \leq 8$ mice, from two independent experiments. **(B)** The non-infected macrophages TNF-α, IL-6 and IL-10 expression was assessed 6 hours after treatment through qPCR analysis. Data was normalized and compared between conditions using the $2^{-\Delta\Delta Cq}$ method. The applied statistical analysis showed statistically significant differences in the TNF-α and IL-6 expression between different meclizine doses. TNF-α – one-way ANOVA ($F(5, 17) = 9.32$, $p < 0.001$); IL-6 – Kruskal-Wallis H test ($X^2(5) = 11.74$, $p = 0.038$); IL-10 – Kruskal-Wallis H test

($X^2(5) = 2.41$, $p = 0.847$). $2 \leq n \leq 4$ mice. **(C)** TNF-α extracellular levels were assessed 2 days post-treatment through ELISA. Kruskal-Wallis H test ($X^2(5) = 8.10$, $p = 0.151$). $3 \leq n \leq 4$ mice.

R.4. Mechanism of action of Meclizine

We know from the literature that meclizine can act through three main cellular pathways, which are directly or indirectly involved in the energetic metabolism of the cell [146, 147, 151-155]. Meclizine is a well-known antihistaminic agent used in the clinic that directly inhibits the activity of the histamine H1 receptor (H1R) [146, 147]. Previous studies have demonstrated its direct regulation of the PFKFB3 levels, thus inducing directly the PFK activity in the glycolytic pathway [146, 152]. And finally, it has been confirmed the meclizine's ability to act on the phosphatidylethanolamine biosynthesis pathway (the ethanolamine branch of the Kennedy Pathway), through direct inhibition of its key enzyme CTP:phosphoethanolamine cytidylyltransferase (PCYT2) [154-156]. This leads to the accumulation of its substrate, phosphoethanolamine, which in higher levels interferes with the mitochondrial oxidative phosphorylation, reducing its activity [155, 156].

With this in mind, we analysed the expression of meclizine direct targets – H1R, PFKFB3, and PCYT2 – at 6 hours after meclizine treatment of *in vitro* infected and non-infected BMDMs (adaptation of the experimental designs represented in **Figures 7** and **10**, respectively). We observed that there were no significant differences in the expression of H1R, and although also non-statistically significant, the PFKFB3 and PCYT2 expression present an apparent increase when infected BMDMs are treated with 40 and 50 μM of meclizine (**Figure 12.A**).

Among these last two meclizine targets, and focusing on glycolysis, we evaluated the direct effect of meclizine on the glycolytic pathway through the inhibition of PFKFB3 activity with the use of its suppressor trimethyl phosphate (3PO). For this, *L. donovani*-infected BMDMs were treated at 2 days post-infection with 40 μM of meclizine, 30 μM of 3PO, the combination of both, 30 μM 3PO combined with DMSO in equivalent volume to the present in 40 μM meclizine solution, or left untreated as control, and on the 4th day post-infection we assessed the parasite load, glucose consumption and lactate production (experimental design adapted from **Figure 7**). We observed no differences between the infected BMDMs treated with meclizine combined with 3PO and the ones treated with meclizine alone (**Figure 12.B** and **12.C**), which indicates that the meclizine effect in this *in vitro* model is not through direct modulation of the glycolytic pathway. Also, no differences were observed in the correspondent non-infected model (**Figure 12.D**).

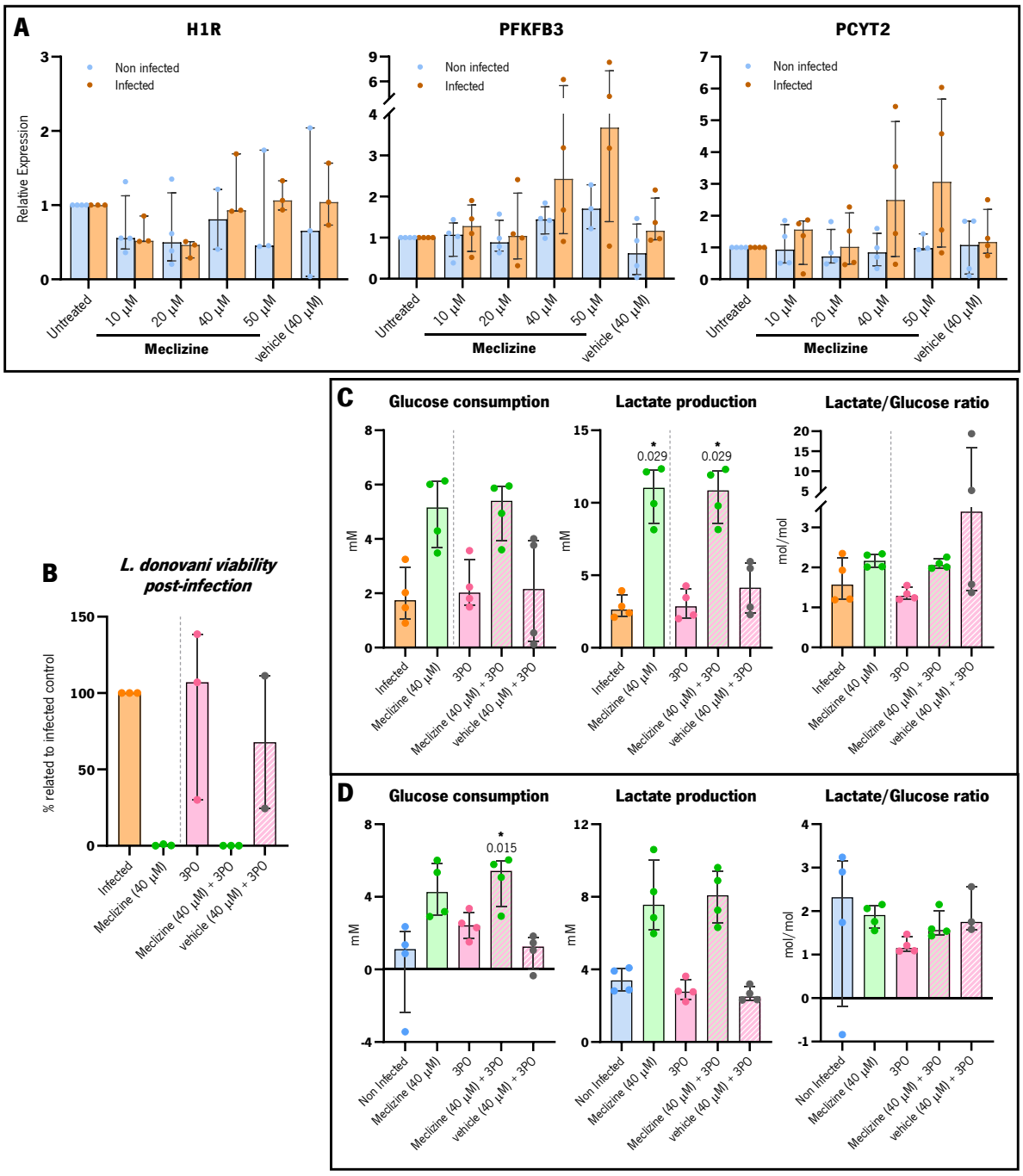

Figure 12. Mechanism of action of Meclizine in the *L. donovani*-infected BMDMs *in vitro* model is not through direct modulation of the glycolytic pathway. (A) Non-infected and *L. donovani*-infected BMDMs were treated at 7 days of M-CSF BMDMs differentiation (non-infected), or at 2 days post-infection (infected), with a dose range of 10 – 50 µM meclizine, treated with DMSO (meclizine's vehicle) in an equivalent volume to 40 µM meclizine, or left untreated as control. At 6h post-treatment, cells total RNA was extracted and the H1R, PFKFB3 and PCYT2 expression was assessed through qPCR analysis. Data was normalized and compared between conditions using the $2^{-\Delta\Delta Cq}$ method. The applied statistical analysis showed a statistically significant difference in the H1R expression in infected BMDMs between different meclizine doses. H1R: Non-infected – Kruskal-Wallis H test ($X^2(5) = 1.68$, $p = 0.891$); Infected – Friedman test ($X^2(5) = 11.00$, $p = 0.019$). PFKFB3: Non-infected – Kruskal-Wallis H test ($X^2(5) = 8.83$, $p = 0.116$); Infected – Friedman test ($X^2(5) = 6.29$, $p = 0.279$). PCYT2:

Non-infected – Kruskal-Wallis H test ($X^2(5) = 1.23$, $p = 0.942$); Infected – Friedman test ($X^2(5) = 7.00$, $p = 0.221$). $2 \leq n \leq 4$ mice. **(B)** *L. donovani*-infected BMDMs were treated at 2 days post-infection with 40 µM meclizine, 30 µM 3PO, 30 µM 3PO + 40 µM meclizine, 3PO + DMSO in equivalent volume to 40 µM meclizine or left untreated as control. On the 4th day post-infection, the parasite load was assessed through PRTA and the number of viable parasites after treatment was normalized against the respective untreated control. The applied Kruskal-Wallis H test showed a statistically significant difference in the number of viable parasites between the different applied treatments ($X^2(4) = 10.21$, $p = 0.006$). $2 \leq n \leq 3$ mice. **(C) and (D)** Glucose consumption and lactate production were assessed on the 4th day post-infection **(C)**, or at 2 days after treatment in non-infected BMDMs **(D)**, through the respective extracellular quantifications by HPLC. The applied Friedman tests showed statistically significant differences in the lactate production of infected and non-infected BMDMs and in the glucose consumption of non-infected BMDMs between the different applied treatments. *(C.1)* Glucose – $X^2(4) = 8.20$, $p = 0.072$; *(C.2)* Lactate – $X^2(4) = 13.40$, $p < 0.001$; (D.1) Glucose – $X^2(4) = 13.60$, $p < 0.001$; (D.2) Lactate – $X^2(4) = 14.60$, $p < 0.001$. The consequent lactate/glucose ratios revealed no statistically significant differences. *(C.3)* Friedman test ($X^2(4) = 8.15$, $p = 0.071$); *(D.3)* Kruskal-Wallis H test ($X^2(4) = 7.17$, $p = 0.127$). **(C) and (D)** n = 4 mice.

R.5. Meclizine as an adjuvant to Miltefosine

According to the data described above in **R.1** to **R.3**, meclizine has a beneficial effect in the context of acute *L. donovani*-infected BMDMs *in vitro* model, with a direct effect in reducing the parasite load starting at 10 µM and having an additional effect on the host macrophage at higher doses (40 to 50 µM). Therefore, we decided to test our second hypothesis, that enhanced glycolysis may improve the currently applied anti-*Leishmania* miltefosine efficacy. However, given that the enhanced glycolytic effect is only observed at higher doses, and that from 10 µM onwards we already observe a meclizine's reducing effect on parasite load, we did not rule out the potential combinatory effect also at these lower doses.

To this end, *in vitro* BMDMs were infected with *L. donovani* and treated at 2 days post-infection with a dose range of 10 to 50 µM meclizine, 2 µM miltefosine, the combination of both, or left untreated as control. On the 4th day post-infection, we assessed the parasite load and macrophage phenotype through their surface markers expression as well as TNF-α secretion (adaptation of the experimental design from **Figure 7**). We observed a synergistic effect between the two treatments in reducing the parasite load, this being statistically significant even at low doses such as 10 µM (**Figure 13.A**). Preliminary data indicated that this synergistic effect may be even more evident with higher doses of meclizine (**Figure 13.B**). Furthermore, we observed that, from 20 µM onwards, there is a dose-dependent increase in the expression of CD86 (not statistically significant), and a dose-dependent reduction in the expression of the markers MHC class II (statistically significant at 50 µM), CD206 and CD301 in the same dose range (20 to 50 µM, not significant) (**Figure 13.C**). We did not observe any differences in the extracellular levels of secreted TNF-α (**Figure 13.D**).

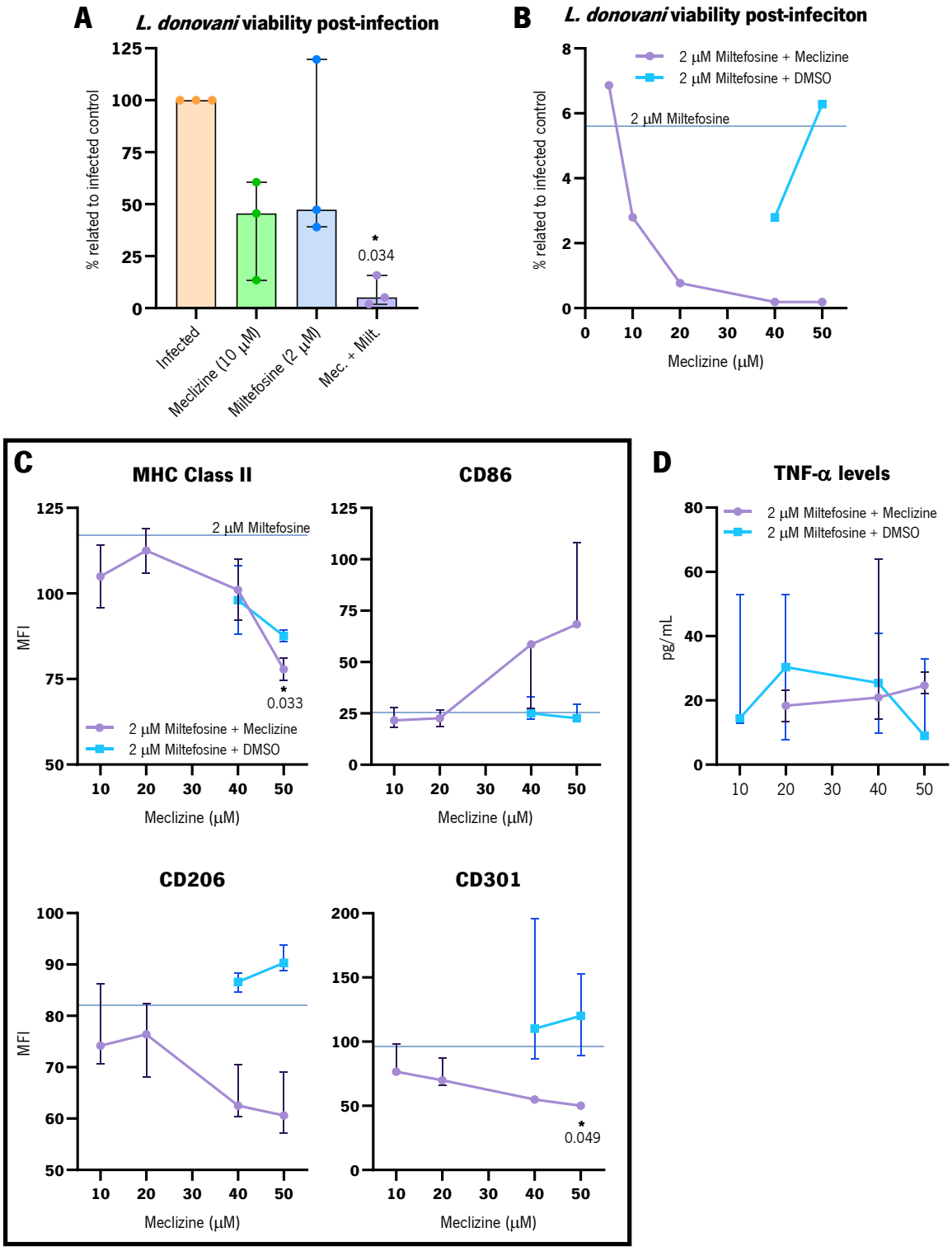

Figure 13. Meclizine and Miltefosine demonstrate a synergic effect on the intracellular parasite load, with an apparent reduction in the host M2-like phenotype and a possible increase in the M1-like phenotype. (A) *L. donovani*-infected BMDMs were treated at 2 days post-infection with 10 μM meclizine, 2 μM miltefosine, the combination of both or left untreated as control. The parasite load was assessed through PRTA and the number of viable *L. donovani* parasites was normalized against the respective untreated control. The applied Friedman test showed a non-statistically significant difference between treatments, $X^2(3)=7.00$, p=0.054. n = 3 mice **(B)** In a similar manner, infected BMDMs were treated at

2 days post-infection with a dose range of 10 µM to 50 µM meclizine, 2 µM miltefosine, the combination of both, or left untreated. On the 4th day post-infection, the parasite load was assessed through PRTA and data normalised against respective untreated control (infected). No statistical analysis was applied, since n = 1 mouse. **(C)** The surface markers expression was assessed through flow cytometry and presented as MFI. The applied Friedman tests showed statistically significant differences in the expression of all markers between applied meclizine doses: MHC class II – $X^2(6) = 12.00$, $p < 0.001$, CD86 – $X^2(6) = 13.34$, $p = 0.038$, CD206 – $X^2(6) = 16.86$, $p = 0.038$, CD301 – $X^2(6) = 16.86$, $p = 0.010$. n = 3 mice **(D)** TNF-α extracellular levels were assessed through ELISA 2 days post-treatment. Kruskal-Wallis H test ($X^2(3) = 3.68$, $p = 0.328$). $2 \leq n \leq 4$ mice.

In summary, these data indicate a synergistic effect between meclizine and miltefosine in reducing the parasite load in the *in vitro* acute infection model in BMDMs. Furthermore, the combinatorial effect of meclizine and miltefosine leads to a suggestive reduction in the surface markers associated with the macrophage M2-like phenotype, and an increase in the expression of the CD86 surface marker, associated with the M1-like phenotype, with a decrease in MHC class II expression. Alongside data from infected BMDMs treated with only a dose range of 10 to 50 µM of meclizine, the combinatorial effect of the two treatments leads to an increase in the CD86 expression, an enhanced reduction of the surface markers CD206 and CD301 expression (**Figure 13.C** vs. **Figure 8.D**), but an apparent inhibition of the meclizine-induced increase of TNF-α levels (**Figure 13.D** vs. **Figure 8.F**). Altogether, the combinatorial treatment of meclizine with miltefosine *in vitro* indicates a potentiated reduction in parasite load, with an apparent reduction in the macrophage M2 phenotype and a possible increase in the M1 phenotype, suggesting an increased host pro-inflammatory response.

R.6. Effect of Meclizine *in vivo*

We observed in **R.2.** that meclizine has a beneficial effect in reducing the acute parasite load *in vitro*, with an apparent polarization preference for the pro-inflammatory phenotype (**Figure 8**). We also observed in **R.5.** that meclizine has a potential synergistic effect with miltefosine in the reduction of acute parasite load *in vitro* (**Figure 13**). And finally, knowing that both compounds have already been tested in mouse models and clinically used in humans, with proven safety, we tried to understand the *in vivo* effect of meclizine, as well as its possible synergistic effect with miltefosine.

For that, BALB/cByJ mice from both sexes were infected intraperitoneally with 1×10^8 *L. donovani* promastigotes, and between days 3 and 7 post-infection, mice were treated with daily 20 mg/kg/day meclizine *per os.*, 20 mg/kg/day miltefosine *per os.*, the combination of both, or with DMSO *per os.* (equivalent volume to the present in meclizine's treatment). On the 10th day post-infection, mice were

euthanised and bone marrow, spleen, liver, and colon were retrieved for further analysis of parasite load and splenocytes population analysis (**Figure 14**).

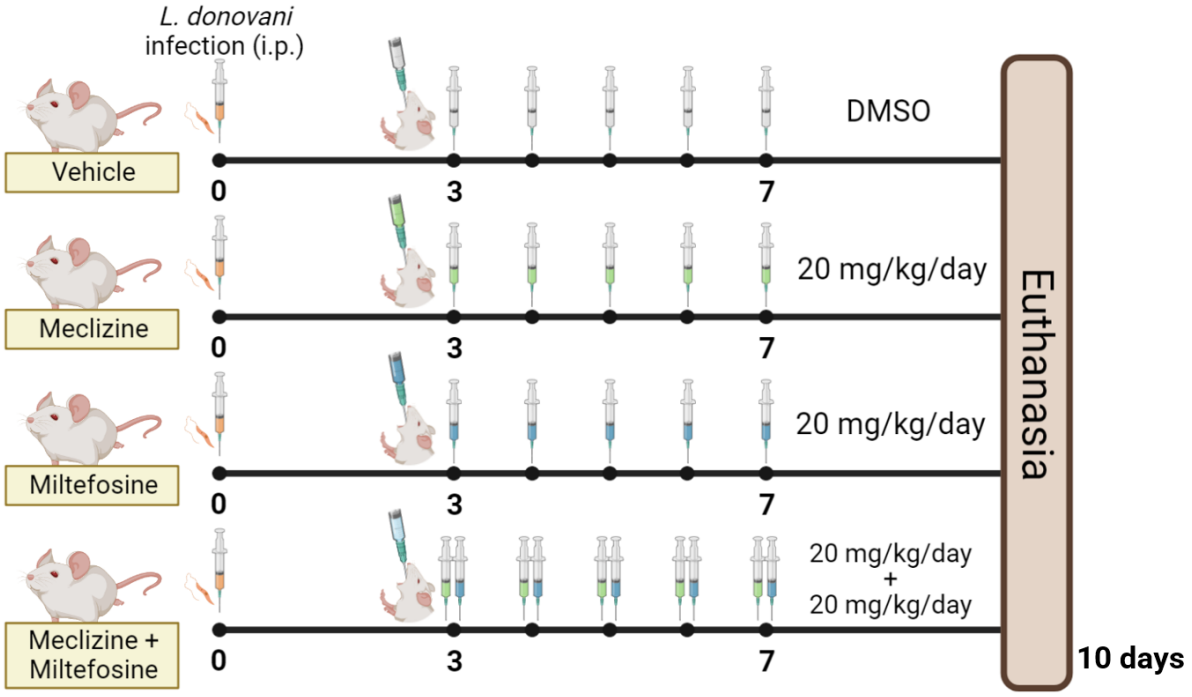

Figure 14. Experimental design *in vivo*. BALB/cByJ male and female mice with 12-14 weeks old were infected with virulent stationary-stage *L. donovani* promastigotes through a single intraperitoneal injection of 1×10^8 promastigotes in 100 µL of apyrogenic PBS 1X (pH 7.4). Between the 3rd and 7th day of *in vivo* infection, mice were treated with daily oral gavages of 20 mg/kg/day of meclizine, 20 mg/kg/day of miltefosine, the combination of both treatments (daily sequential administrations) or treated with 50% v/v of DMSO in apyrogenic PBS as meclizine's vehicle control. On the 10th day of infection, mice were euthanized by carbon dioxide (CO_2) inhalation, followed by cervical dislocation to confirm death, and the spleen, liver, bone marrow and colon were retrieved for subsequent assessment of *L. donovani* burden present in each organ by quantitative polymerase chain reaction (qPCR) analysis of total DNA, and for immune cells' phenotypical analysis (spleen) by flow cytometry.

We observed a significant reduction in bone marrow and spleen parasite load when mice were treated with miltefosine or with the combination of both treatments (**Figure 15.A**). We also observed a significant increase in the liver parasite load when mice were treated with meclizine alone, and a non-significant reduction in this organ's parasite load when treated with miltefosine (**Figure 15.A**). We did not observe any differences in the colon's parasite load (**Figure 15.A**). Furthermore, we analyse the T cell populations present in mice spleens and we did not observe any significant difference in $CD4^+$ or $CD8^+$ T cell populations, nor in their percentage of naïve ($CD62L^+CD44^-$) or effector cells ($CD44^+$), with the latter being the ones already induced and activated by APCs' antigen presentation (**Figure 15.B**).

Despite the increase in parasite load in the liver when mice were treated with meclizine alone, overall, these data show no significant changes in the parasite load induced by meclizine, neither applied alone nor in combination with miltefosine (even when compared to miltefosine alone). Thus, since meclizine did not appear to enhance the effect of miltefosine (in parasite load nor in T cell populations percentage), we did not proceed with further characterization of the host immune response.

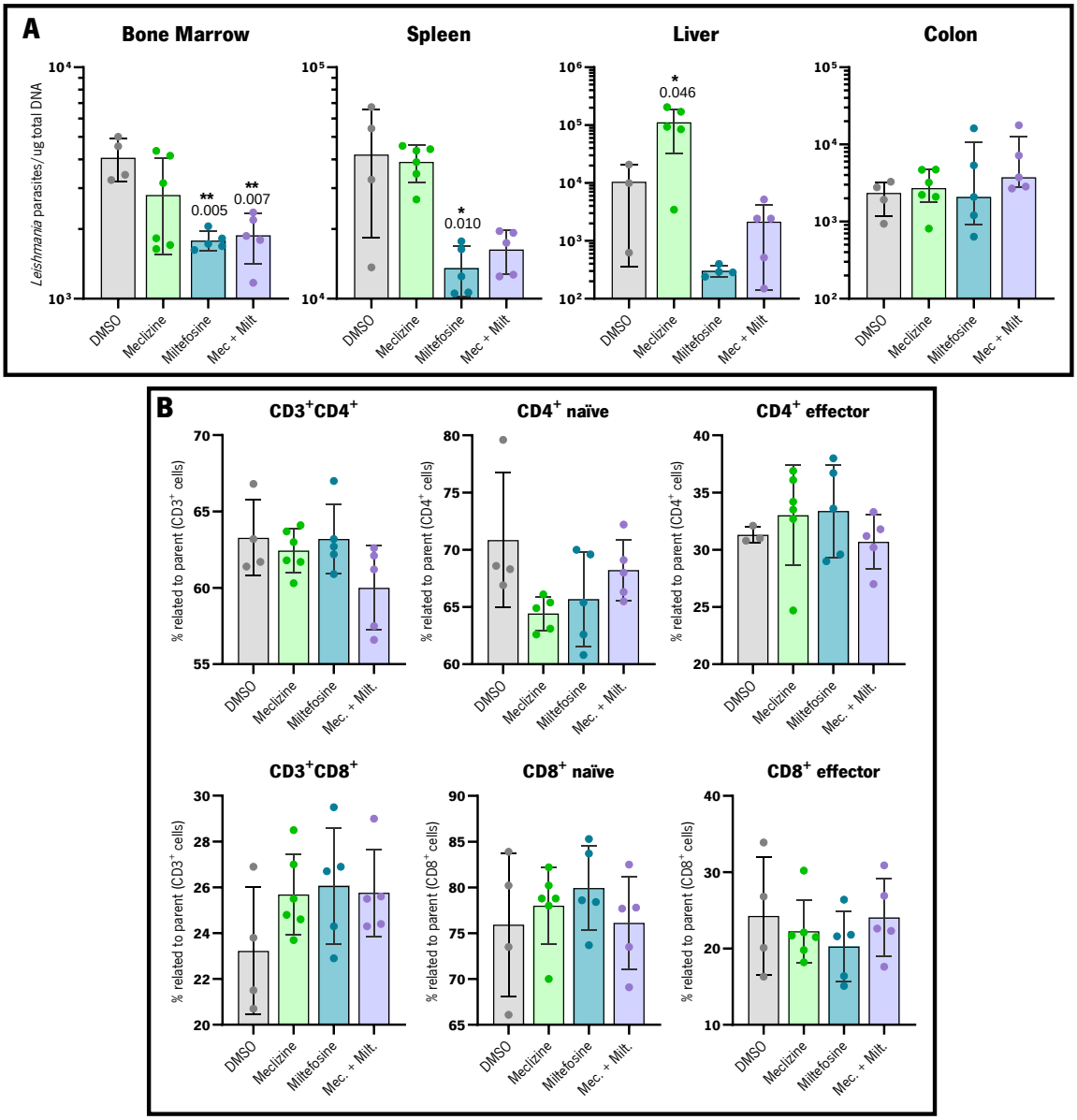

Figure 15. Meclizine did not induce a reduction in the organs parasite load nor induced significant changes in the T cells sub-populations percentage. (A) *L. donovani*-infected BALB/cByJ mice, between the 3rd and 7th day post-infection were treated with 20 mg/kg/day meclizine, 20 mg/kg/day miltefosine, the combination of both treatments, or treated with 50% v/v DMSO. On the 10th day post-infection, mice were euthanized, the organs were retrieved, and the parasite load was assessed through qPCR quantifications of *Leishmania* kinetoplastid DNA. The applied one-way ANOVAs showed statistically significant differences between treatments in the parasite load quantified in the bone marrow, spleen, and liver. Bone marrow – $F(3, 20) = 7.15$, $p = 0.003$; Spleen – $F(3, 20) = 8.48$, $p = 0.001$; Liver – $F(3, 17) = 7.12$, $p = 0.004$; Colon

– $F(3, 20) = 0.980$, $p = 0.427$. $4 \leq n \leq 6$ mice **(B)** The splenocytes from infected and treated mice were analysed by flow cytometry, and data is presented as percentage related to the respective parent population. The applied statistical analysis showed no statistically significant differences between treatments in any analysed T cell population. $CD4^+$ T cells: one-way ANOVA – $F(3, 20) = 2.28$, $p = 0.119$; $CD4^+$ naïve T cells: Kruskal-Wallis test – $X^2(3) = 7.01$, $p = 0.072$; $CD4^+$ effector T cells: Kruskal-Wallis test – $X^2(3) = 3.10$, $p = 0.401$; $CD8^+$ T cells: one-way ANOVA – $F(3, 20) = 1.48$, $p = 0.257$; $CD8^+$ naïve T cells: Kruskal-Wallis test – $X^2(3) = 2.18$, $p = 0.536$; $CD8^+$ effector T cells: Kruskal-Wallis test – $X^2(3) = 2.38$, $p = 0.497$. $4 \leq n \leq 6$ mice.

DISCUSSION

The host-pathogen metabolic interaction is crucial for the outcome of infection, defining parasite invasion and host protective strategies. The host immune system has several mechanisms that confer protection against different invading pathogens without compromising the integrity of the host itself [55, 56]. However, we and others have demonstrated that *Leishmania* infection induces profound alterations in the host cell metabolism, promoting intracellular parasite survival and consequent maintenance of chronic infections [57, 129, 134, 157-159]. In acute VL infections, glycolysis is the main energy source for rapid immune system activation and efficient pro-inflammatory response [77, 102]. In neutrophils and macrophages, the presence of parasites drives them into a Warburg-like response, with increased glycolysis to rapidly resolve the infection [66, 67, 135].

Previous work from our group has shown that the inhibition of host glycolysis *in vitro* retracted important macrophage and neutrophils functions crucial for infection control and that the same inhibition *in vivo* prior to *Leishmania* infection leads to increased host susceptibility and increased parasite burden [138]. As no other studies are known to focus on the effect of increased glycolysis in the context of VL infection, our first hypothesis was whether increased glycolysis can promote parasite clearance. To this end, and focusing on objective 1.a, we tested in the context of *in vitro* infection compounds that modulate glycolysis through direct action on glycolytic enzymes or by modulation of elevated HIF-1α levels [130, 145-147]. HIF-1α is an indicator of hypoxic conditions, such as those present in granulomas of acute *Leishmania* infections, and among other pathways, upregulates glycolysis to ensure cell survival [84, 131, 134]. As such, daprodustat, DMOG, FG-2216, and roxadustat are inhibitors of HIFs prolyl 4-hydroxylases, stabilize increased HIF-1α levels, and were therefore chosen for the screening [130]. In turn, alfuzosin and terazosin were selected for their direct action on glycolysis by potentiating PGK1 activity, and similarly, meclizine was chosen for activating the glycolytic enzyme PFK through increased levels of PFKFB3 [145-147].

In both analysed treatment timepoints, the tested compounds showed opposite effects on the evolution of the acute *L. donovani*-infected BMDMs parasite load. HIFs prolyl 4-hydroxylases inhibitors led to an increase in parasite load, enhancers of the PGK1 activity did not show a clear trend in the evolution of parasite load, and the inducer of increased PFKFB3 levels, with consequent PFK activation, induced a significant reduction in parasite load (**Figure 5**). This drug screening is based on preliminary data, where stabilizers of elevated HIF-1α levels are only represented by data retrieved from a single mouse BMDMs (although being representative of what was observed in data from 3 different mice). Therefore, this experiment should be repeated and possibly consider testing other doses, since previous studies that

describe these compounds as glycolysis enhancers, were performed with different cell cultures (with cell-specific drug sensitivities) and tested in clinical trials [130, 145-147], so the apparently contradictory data may be merely the result of the doses applied.

Given that meclizine demonstrated the best-reducing effect on intracellular parasite load, and focusing on objectives 1.b and 1.c, we performed *in vitro* meclizine dose-response assays on host immune system cell activation, its pro-inflammatory response, glycolytic activity, and parasite clearance. To this end, *in vitro L. donovani*-infected BMDMs were treated 2 days post-infection with a dose range of 0.1 to 50 μM of meclizine. It was possible to calculate a meclizine IC_{50} against *L. donovani* of 13.15 μM, with 95% CI from 7.31 to 25.66 μM (**Figure 8.A**). Is noteworthy the visible variability in the percentage of parasite viability between BMDMs from different mice when treated with the same dose of meclizine. This can also be partially explained by the inherent limitations of the technique applied here. The PRTA technique is based on the promotion of a hypoxic environment at temperatures favourable for the parasite (26°C) and stressful for the host cell, to promote macrophage bursting and conversion of amastigotes into promastigotes [142]. The possible presence of occasional external stressors (variations in pH, temperature, etc.) causes macrophages not to burst and/or amastigotes not to convert into promastigotes, leading to an erroneous underestimation of parasite viability and inducing variability even between experimental replicates. Alternatively, it is possible to stain the intracellular parasite and analyse the infection by the number of infected and non-infected macrophages and the number of parasites per macrophage [160, 161]. However, this technique is more time-consuming and is not able to distinguish viable from non-viable parasites, which is an advantage of the PRTA technique, where only viable parasites are counted. Nonetheless, the observed variability in *L. donovani* viability in infected BMDMs affects the accuracy of the IC_{50} calculation, and since the present data analysis was performed based on 4 to 6 mice, repetition of this experiment will allow a reduction of the inter-mice variability effect and a more accurate measurement of the meclizine IC_{50} against intracellular *L. donovani*.

Alongside the parasite and macrophage viability analysis, we assessed the host cell glycolytic activity by quantifying the glucose consumption and lactate production by HPLC. We observed significant increases in both parameters when cells are treated with meclizine doses higher than 10 μM (**Figure 8.C**). However, the consequent lactate/glucose ratio presented high interquartile range when compared to each parameter analysis and exhibit non-glycolytic ratios of 3 mol/mol, even after outliers' removal. This can be explained by the fact that, in the biological context, glucose consumed by cells may not be entirely directed to the glycolytic pathway and be used in the glycogen and acetyl coenzyme A synthesis [162, 163]. Also, the intracellular production of glucose through gluconeogenesis can occur, reducing the

uptake of extracellular glucose by the cell [163]. On the opposite side, intracellular lactate, instead of being secreted, can be converted into pyruvate and H^+ for reconversion into glucose through gluconeogenesis [163, 164]. In addition, lactate can come from sources other than glucose, such as glycogen [164]. This misleading reduction in glucose uptake and/or lactate secretion masks the analysis of possible variations in the glycolytic pathway activity. Alternatively, it is possible to analyse the energy metabolism of the host cell by measuring the rate of extracellular acidification (ECAR) alongside the rate of oxygen consumption (OCR) [165]. These are direct indicators of the glycolytic pathway activity and oxidative phosphorylation, respectively, and the ECAR/OCR ratio allows the identification of the cells' energetic activity and by which of these pathways it is more metabolically active [165]. However, this is a more expensive technique and considering the high number of samples analysed in the context of this work, the glycolysis analysis by HPLC turned out to be the most adequate.

We know from the literature that CD206 and CD301 surface markers expression is associated with the more *Leishmania* permissive M2-like phenotype, while the CD86 expression and increased MHC class II expression are associated with the pro-inflammatory M1-like phenotype [148-150]. With increasing doses of meclizine, we did not observe evident differences in the expression of these markers, except for CD301, which significantly reduced its expression with 40 μM of meclizine (**Figure 8.D**). Considering that, simultaneously, we observed a gradual increase in the expression of TNF-α and consequent accumulation of this cytokine in the extracellular environment (**Figure 8.E and 8.F**), and knowing from the literature that this is associated with the pro-inflammatory profile of macrophages [5, 79, 80], the suggestive increase in the M1 phenotype will have to be confirmed by repeating these experiments, in particular the analysis of surface markers.

To clarify whether the reduction of the parasite load is through the host's pro-inflammatory immune response and/or by direct toxicity for the parasite (objective 1.d), we tested the latter by treating axenic *L. donovani* cultures with meclizine and used non-infected macrophages to tackle the effect of meclizine on the macrophage itself. Axenic cultures of *L. donovani* were cultured with doses from 0.1 to 50 μM of meclizine and during the following 9 days demonstrated a dose-dependent and directly proportional growth impairment (**Figure 9**). What we observed in these cultures is consistent with previous studies, where de Melo Mendes *et al.* demonstrated a direct parasiticidal effect of meclizine in *L. infantum* promastigotes, with an IC_{50} of 27.84 μM after 24 hours of co-culture and an IC_{50} of 17.30 μM after 48 hours of co-culture with meclizine [151]. However, to confirm if the leishmanicidal effect is maintained (and at the same doses) in the *in vitro* infection model of *L. donovani*-infected BMDMs, the meclizine-

Leishmania interaction should also be tested with axenic amastigotes, as a bridge between the two *in vitro* models discussed here.

In turn, non-infected BMDMs were treated with meclizine doses from 0.1 to 50 μM, and after 2 days post-treatment, they demonstrated a significant increase in the CD86 expression when treated with 50 μM of meclizine, and an apparent dose-dependent reduction in the CD301 expression (**Figure 11.A**). We also observed a significant increase in the TNF-α expression with increasing doses of meclizine, with no apparent changes in the extracellular levels of this cytokine (**Figure 11.B and 11.C**). These data are in accordance with an increase in macrophage polarization towards the M1 phenotype with increasing doses of meclizine. However, as the M1 phenotype is associated with increased glycolytic activity [77, 102], this should also be confirmed by analysing this pathway under these conditions.

Knowing from the literature that meclizine can act through three distinct metabolic pathways, and that these are directly or indirectly associated with the energy metabolism of the cell [146, 147, 151-155], it is important to understand by which of these pathways it exerts its effect. We evaluated the expression of meclizine direct targets (H1R, PFKFB3, and PCYT2) in each pathway at 6 hours after meclizine treatment of infected BMDMs. We only observed an apparent increase in the expression of the meclizine targets involved in the glycolytic pathway and in the phosphatidylethanolamine biosynthesis pathway (**Figure 12.A**). With glycolysis being the focus of this study, we chose to test firstly the direct effect of meclizine on glycolysis by inhibition of PFKFB3 with 3PO. We did not observe any differences in the effect of meclizine on the host cell glycolytic activity nor upon the elimination of the intracellular parasite load (**Figure 12.B to D**). This leads us to conclude that the effect of meclizine is not through direct action on glycolysis. On the other hand, meclizine also acts on the key enzyme of the phosphatidylethanolamine biosynthesis pathway, which also showed an apparent increase in expression upon infection and treatment. In this pathway, meclizine inhibits the activity of PCYT2, leading to the accumulation of its substrate phosphoethanolamine [154-156]. The latter, at high levels, interferes with the mitochondrial oxidative phosphorylation, which reduces its activity and, consequently, the cell's energy metabolism becomes more dependent on the glycolytic pathway. This also supports the increased glycolytic activity, and consequent M1 macrophage polarization suggested by the data described above (**Figures 8 and 11**).

To confirm this possibility, future studies will have to address the direct effect of meclizine on the phosphatidylethanolamine biosynthesis pathway in the context of VL infection. Furthermore, although we did not observe differences in the H1R expression, we cannot discard the possible effect of meclizine on the histamine signalling pathway in the context of VL infection. Histamine is described as an enhancer of the macrophage M2 polarization and inhibitor of TNF-α secretion, with the H1R signalling pathway

inducing the M2-like phenotype in tumour-associated macrophages and suppressing the $CD8^+$ T cell function [166-169].

Considering the beneficial effects of meclizine in the acute *L. donovani* infection model *in vitro*, and to be able to transfer to the *in vivo* model (objective 2), we tested *in vitro* our second hypothesis with the possible combinatory effect of meclizine with the already applied anti-*Leishmania* miltefosine. *L. donovani*-infected BMDMs were treated at 2 days post-infection with miltefosine, a dose range of 10 to 50 μM meclizine, the combination of both, or left untreated. We observed a significant synergistic effect between treatments in reducing the parasite load, and a suggestive combinatory effect in the increased expression of CD86 and reduction of both CD206 and CD301 surface markers (**Figure 13**). This indicates a promotion of the M1-like macrophage phenotype and a reduction of the M2-like phenotype. In this manner, the macrophage population presents a more pro-inflammatory phenotype and is capable of further reducing the parasite load. However, these are only preliminary data and will need to be repeated to confirm these observed pro-inflammatory and parasite clearance tendencies.

Nonetheless, knowing that both compounds have already been tested in mouse models and are clinically used in humans, being safe, and considering the potential beneficial effect, we translated to the *in vivo* mouse model of BALB/cByJ mice infected with *L. donovani* and treated with 20 mg/kg/day of meclizine *per os*, 20 mg/kg/day of miltefosine *per os*, the combination of both, or treated with meclizine's vehicle as the control group. Compared with the control group, we did not observe a reduction in the parasite load (in any of the organs analysed) when mice were treated with meclizine alone (**Figure 15.A**, objective 2.a). Furthermore, the combination of both treatments did not differ from the effect induced by miltefosine alone in the parasite load (**Figure 15.A**, objective 2.b). Also, no differences were observed in the percentage of $CD4^+$ or $CD8^+$ T cells populations, indicative of the T_h and T_{reg}, or T_c presence in the spleen, respectively (**Figure 14.B**). Thus, since meclizine did not appear to enhance the effect of miltefosine, we did not proceed with further characterization of the host immune response.

Compared with *in vitro* data (**Figure 8**), the lack of differences observed in the parasite load when mice were treated with meclizine may be due to the dose applied in the *in vivo* model, which may not be the most appropriate for the reductive effect observed *in vitro*. On the other hand, since meclizine was dissolved in DMSO, which itself has a systemic effect in mice [170] and a direct effect on the parasite load *in vitro* (data not shown), we do not know whether this may be masking the *in vivo* data. Therefore, future *in vivo* experiments must consider meclizine dissolved in another non-polar solvent (e.g. corn oil) and consider the use of other meclizine concentrations to test the dose effect on the parasite burden *in vivo*.

CONCLUDING REMARKS AND FUTURE PERSPECTIVES

In conclusion, we saw that meclizine presents a beneficial effect in reducing the acute parasite load *in vitro*, with an additional effect at higher doses on the host macrophage's glycolysis, associated with the macrophage polarization towards the M1 glycolytic pro-inflammatory phenotype. This differential dose effect can be partially explained by the direct meclizine's toxicity on the parasite (10 μM onwards) and by the pro-glycolytic effect on the host macrophage (40 to 50 μM), with the latter being potentiated in the context of *L. donovani* infection. Furthermore, we observed that meclizine has an *in vitro* synergistic effect with the currently orally available miltefosine, with the potential to be explored *in vivo*. However, these experiments must be repeated to confirm the observed dose-dependent, and combinatory effects, on the pro-inflammatory and parasite clearance tendencies.

Also, knowing from the literature that meclizine can act on host cell metabolism by (1) modulating histamine signalling through H1R, (2) direct effect on glycolysis through increased PFKFB3 levels and/or (3) truncating the phosphatidylethanolamine biosynthesis pathway in the PCYT2 enzyme, we demonstrate that the effect of meclizine on the *in vitro* system under study is not through direct action on glycolysis. Future experiments will unfold the exact mechanism by which meclizine exerts its effect on the host pro-inflammatory phenotype and the importance of glycolysis enhancement on the host immune response and control of the intracellular parasite load.

Overall, this will allow us to address a possible immunotherapeutic adjuvant for the existing first-line anti-*Leishmania* therapeutics efficacy and improve VL patients' treatment.

REFERENCES

1. Bodhale N, Ohms M, Ferreira C, Mesquita I, Mukherjee A, André S, et al. Cytokines and metabolic regulation: A framework of bidirectional influences affecting Leishmania infection. Cytokine. 2021;147:155267.

2. Burza S, Croft SL, Boelaert M. Leishmaniasis. The Lancet. 2018;392(10151):951-70.

3. Murray HW, Berman JD, Davies CR, Saravia NG. Advances in leishmaniasis. The Lancet. 2005;366(9496):1561-77.

4. Saha B, Silvestre R. Cytokines in the immunity and immunopathogenesis in leishmaniases. Cytokine. 2020;145:155320.

5. Saunders EC, McConville MJ. Immunometabolism of *Leishmania* granulomas. Immunol Cell Biol. 2020;98(10):832-44.

6. WHO. Weekly Epidemiological Record, 2020, vol. 95, 25. Weekly Epidemiological Record. 2020;95(25):265-80.

7. WHO. Weekly Epidemiological Record, 2021, vol. 96, 35. Weekly Epidemiological Record. 2021;96(35):401-20.

8. Gradoni L, López-Vélez R, Mokni M. Manual on case management and surveillance of the leishmaniases in the WHO European Region. Copenhagen: World Health Organization. Regional Office for Europe; 2017 2017.

9. Colmenares M, Kar S, Goldsmith-Pestana K, McMahon-Pratt D. Mechanisms of pathogenesis: differences amongst *Leishmania* species. Trans R Soc Trop Med Hyg. 2002;96 Suppl 1:S3-7.

10. de Vries HJC, Reedijk SH, Schallig HDFH. Cutaneous Leishmaniasis: Recent Developments in Diagnosis and Management. American Journal of Clinical Dermatology. 2015;16(2):99-109.

11. Cincurá C, de Lima CMF, Machado PRL, Oliveira-Filho J, Glesby MJ, Lessa MM, et al. Mucosal leishmaniasis: A Retrospective Study of 327 Cases from an Endemic Area of *Leishmania* (Viannia) braziliensis. Am J Trop Med Hyg. 2017;97(3):761-6.

12. Fikre H, Mohammed R, Atinafu S, van Griensven J, Diro E. Clinical features and treatment response of cutaneous leishmaniasis in North-West Ethiopia. Tropical Medicine & International Health. 2017;22(10):1293-301.

13. Guerra JAdO, Prestes SR, Silveira H, Coelho LIdARC, Gama P, Moura A, et al. Mucosal Leishmaniasis Caused by *Leishmania* (Viannia) *braziliensis* and *Leishmania* (Viannia) *guyanensis* in the Brazilian Amazon. PLOS Neglected Tropical Diseases. 2011;5(3):e980.

14. Saini I, Joshi J, Kaur S. Unwelcome prevalence of leishmaniasis with several other infectious diseases. Int Immunopharmacol. 2022;110:109059.

15. Olivier M, Badaró R, Medrano FJ, Moreno J. The pathogenesis of *Leishmania*/HIV co-infection: cellular and immunological mechanisms. Annals of Tropical Medicine & Parasitology. 2003;97(sup1):79-98.

16. Adriaensen W, Dorlo TPC, Vanham G, Kestens L, Kaye PM, van Griensven J. Immunomodulatory Therapy of Visceral Leishmaniasis in Human Immunodeficiency Virus-Coinfected Patients. Front Immunol. 2017;8:1943.

17. Diro E, Edwards T, Ritmeijer K, Fikre H, Abongomera C, Kibret A, et al. Long term outcomes and prognostics of visceral leishmaniasis in HIV infected patients with use of pentamidine as secondary prophylaxis based on CD4 level: a prospective cohort study in Ethiopia. PLOS Neglected Tropical Diseases. 2019;13(2):e0007132.

18. Cloots K, Marino P, Burza S, Gill N, Boelaert M, Hasker E. Visceral Leishmaniasis-HIV Coinfection as a Predictor of Increased *Leishmania* Transmission at the Village Level in Bihar, India. Front Cell Infect Microbiol. 2021;11:604117.

19. Ready PD. Epidemiology of visceral leishmaniasis. Clin Epidemiol. 2014;6:147-54.

20. Abdoli A, Maspi N, Ghaffarifar F, Nasiri V. Viscerotropic leishmaniasis: a systematic review of the case reports to highlight spectrum of the infection in endemic countries. Parasitology Open. 2018;4:e11.

21. Zijlstra EE. The immunology of post-kala-azar dermal leishmaniasis (PKDL). Parasit Vectors. 2016;9(1):464.

22. Boelaert M, Meheus F, Sanchez A, Singh SP, Vanlerberghe V, Picado A, et al. The poorest of the poor: a poverty appraisal of households affected by visceral leishmaniasis in Bihar, India. Tropical Medicine & International Health. 2009;14(6):639-44.

23. Burza S, Mahajan R, Sinha PK, van Griensven J, Pandey K, Lima MA, et al. Visceral leishmaniasis and HIV co-infection in Bihar, India: long-term effectiveness and treatment outcomes with liposomal amphotericin B (AmBisome). PLoS Negl Trop Dis. 2014;8(8):e3053.

24. Stauch A, Duerr HP, Dujardin JC, Vanaerschot M, Sundar S, Eichner M. Treatment of visceral leishmaniasis: model-based analyses on the spread of antimony-resistant *L. donovani* in Bihar, India. PLoS Negl Trop Dis. 2012;6(12):e1973.

25. Chowdhury R, Mondal D, Chowdhury V, Faria S, Alvar J, Nabi SG, et al. How Far Are We from Visceral Leishmaniasis Elimination in Bangladesh? An Assessment of Epidemiological Surveillance Data. PLOS Neglected Tropical Diseases. 2014;8(8):e3020.

26. Sundar S, Chakravarty J. Leishmaniasis: an update of current pharmacotherapy. Expert Opinion on Pharmacotherapy. 2013;14(1):53-63.

27. Jha TK, Giri YN, Singh TK, Jha S. Use of amphotericin B in drug-resistant cases of visceral leishmaniasis in north Bihar, India. Am J Trop Med Hyg. 1995;52(6):536-8.

28. Kumari S, Kumar V, Tiwari RK, Ravidas V, Pandey K, Kumar A. Amphotericin B: A drug of choice for Visceral Leishmaniasis. Acta Tropica. 2022;235:106661.

29. Thakur CP, Ahmed S. Observations on amphotericin B treatment of kala-azar given in a rural set up in Bihar, India. Indian J Med Res. 2001;113:14-8.

30. Singh OP, Singh B, Chakravarty J, Sundar S. Current challenges in treatment options for visceral leishmaniasis in India: a public health perspective. Infectious Diseases of Poverty. 2016;5(1):19.

31. Saravolatz LD, Bern C, Adler-Moore J, Berenguer J, Boelaert M, den Boer M, et al. Liposomal Amphotericin B for the Treatment of Visceral Leishmaniasis. Clinical Infectious Diseases. 2006;43(7):917-24.

32. Sundar S, Chakravarty J, Agarwal D, Rai M, Murray HW. Single-dose liposomal amphotericin B for visceral leishmaniasis in India. N Engl J Med. 2010;362(6):504-12.

33. Das VN, Ranjan A, Sinha AN, Verma N, Lal CS, Gupta AK, et al. A randomized clinical trial of low dosage combination of pentamidine and allopurinol in the treatment of antimony unresponsive cases of visceral leishmaniasis. J Assoc Physicians India. 2001;49:609-13.

34. Diro E, Ritmeijer K, Boelaert M, Alves F, Mohammed R, Abongomera C, et al. Use of Pentamidine As Secondary Prophylaxis to Prevent Visceral Leishmaniasis Relapse in HIV Infected Patients, the First Twelve Months of a Prospective Cohort Study. PLoS Negl Trop Dis. 2015;9(10):e0004087.

35. Diro E, Ritmeijer K, Boelaert M, Alves F, Mohammed R, Abongomera C, et al. Long-term Clinical Outcomes in Visceral Leishmaniasis/Human Immunodeficiency Virus-Coinfected Patients During and After Pentamidine Secondary Prophylaxis in Ethiopia: A Single-Arm Clinical Trial. Clin Infect Dis. 2018;66(3):444-51.

36. Seaman J, Pryce D, Sondorp HE, Moody A, Bryceson AD, Davidson RN. Epidemic visceral leishmaniasis in Sudan: a randomized trial of aminosidine plus sodium stibogluconate versus sodium stibogluconate alone. J Infect Dis. 1993;168(3):715-20.

37. Sundar S, Jha TK, Thakur CP, Sinha PK, Bhattacharya SK. Injectable paromomycin for Visceral leishmaniasis in India. N Engl J Med. 2007;356(25):2571-81.

38. Dorlo TP, Balasegaram M, Beijnen JH, de Vries PJ. Miltefosine: a review of its pharmacology and therapeutic efficacy in the treatment of leishmaniasis. J Antimicrob Chemother. 2012;67(11):2576-97.

39. Dorlo TP, Huitema AD, Beijnen JH, de Vries PJ. Optimal dosing of miltefosine in children and adults with visceral leishmaniasis. Antimicrob Agents Chemother. 2012;56(7):3864-72.

40. Olliaro PL, Guerin PJ, Gerstl S, Haaskjold AA, Rottingen J-A, Sundar S. Treatment options for visceral leishmaniasis: a systematic review of clinical studies done in India, 1980-2013;2004. The Lancet Infectious Diseases. 2005;5(12):763-74.

41. van Griensven J, Balasegaram M, Meheus F, Alvar J, Lynen L, Boelaert M. Combination therapy for visceral leishmaniasis. Lancet Infect Dis. 2010;10(3):184-94.

42. Thakur CP, Kumar M, Pandey AK. Comparison of regimes of treatment of antimony-resistant kala-azar patients: a randomized study. Am J Trop Med Hyg. 1991;45(4):435-41.

43. Sundar S, Sinha PK, Rai M, Verma DK, Nawin K, Alam S, et al. Comparison of short-course multidrug treatment with standard therapy for visceral leishmaniasis in India: an open-label, non-inferiority, randomised controlled trial. Lancet. 2011;377(9764):477-86.

44. Ferreira C, Mesquita I, Barbosa AM, Osório NS, Torrado E, Beauparlant CJ, et al. Glutamine supplementation improves the efficacy of miltefosine treatment for visceral leishmaniasis. PLoS Negl Trop Dis. 2020;14(3):e0008125.

45. Dey S, Mukherjee D, Sultana SS, Mallick S, Dutta A, Ghosh J, et al. Combination of *Mycobacterium indicus pranii* and Heat-Induced Promastigotes Cures Drug-Resistant Leishmania Infection: Critical Role of Interleukin-6-Producing Classical Dendritic Cells. Infect Immun. 2020;88(6).

46. Joshi J, Kaur S. To investigate the therapeutic potential of immunochemotherapy with cisplatin + 78 kDa + MPL-A against *Leishmania donovani* in BALB/c mice. Parasite Immunol. 2014;36(1):3-12.

47. Killick-Kendrick R. The life-cycle of *Leishmania* in the sandfly with special reference to the form infective to the vertebrate host. Ann Parasitol Hum Comp. 1990;65 Suppl 1:37-42.

48. Bates PA. Transmission of *Leishmania* metacyclic promastigotes by phlebotomine sand flies. Int J Parasitol. 2007;37(10):1097-106.

49. Rosenzweig D, Smith D, Opperdoes F, Stern S, Olafson RW, Zilberstein D. Retooling *Leishmania* metabolism: from sand fly gut to human macrophage. Faseb j. 2008;22(2):590-602.

50. McConville MJ, de Souza D, Saunders E, Likic VA, Naderer T. Living in a phagolysosome; metabolism of *Leishmania* amastigotes. Trends in Parasitology. 2007;23(8):368-75.

51. McConville MJ, Saunders EC, Kloehn J, Dagley MJ. *Leishmania* carbon metabolism in the macrophage phagolysosome- feast or famine? F1000Research. 2015;4(F1000 Faculty Rev):938.

52. Young J, Kima PE. The *Leishmania* Parasitophorous Vacuole Membrane at the Parasite-Host Interface. Yale J Biol Med. 2019;92(3):511-21.

53. Bañuls AL, Hide M, Prugnolle F. *Leishmania* and the leishmaniases: a parasite genetic update and advances in taxonomy, epidemiology and pathogenicity in humans. Adv Parasitol. 2007;64:1-109.

54. Kamhawi S. Phlebotomine sand flies and *Leishmania* parasites: friends or foes? Trends Parasitol. 2006;22(9):439-45.

55. Koenderman L, Buurman W, Daha MR. The innate immune response. Immunol Lett. 2014;162(2 Pt B):95-102.

56. Carrillo JLM, García FPC, Coronado ÓG, García MAM, Cordero JFC, editors. Physiology and Pathology of Innate Immune Response Against Pathogens. 2017.

57. Martínez-López M, Soto M, Iborra S, Sancho D. *Leishmania* Hijacks Myeloid Cells for Immune Escape. Front Microbiol. 2018;9:883.

58. Brinkmann V, Reichard U, Goosmann C, Fauler B, Uhlemann Y, Weiss DS, et al. Neutrophil extracellular traps kill bacteria. Science. 2004;303(5663):1532-5.

59. McDonald B, Urrutia R, Yipp BG, Jenne CN, Kubes P. Intravascular neutrophil extracellular traps capture bacteria from the bloodstream during sepsis. Cell Host Microbe. 2012;12(3):324-33.

60. Yipp BG, Petri B, Salina D, Jenne CN, Scott BN, Zbytnuik LD, et al. Infection-induced NETosis is a dynamic process involving neutrophil multitasking *in vivo*. Nat Med. 2012;18(9):1386-93.

61. Pilsczek FH, Salina D, Poon KKH, Fahey C, Yipp BG, Sibley CD, et al. A Novel Mechanism of Rapid Nuclear Neutrophil Extracellular Trap Formation in Response to *Staphylococcus aureus*. The Journal of Immunology. 2010;185(12):7413-25.

62. Yizengaw E, Getahun M, Tajebe F, Cruz Cervera E, Adem E, Mesfin G, et al. Visceral Leishmaniasis Patients Display Altered Composition and Maturity of Neutrophils as well as Impaired Neutrophil Effector Functions. Front Immunol. 2016;7:517.

63. Gabriel C, McMaster WR, Girard D, Descoteaux A. *Leishmania donovani* Promastigotes Evade the Antimicrobial Activity of Neutrophil Extracellular Traps. The Journal of Immunology. 2010;185(7):4319-27.

64. Guimarães-Costa AB, DeSouza-Vieira TS, Paletta-Silva R, Freitas-Mesquita AL, Meyer-Fernandes JR, Saraiva EM. 3'-nucleotidase/nuclease activity allows *Leishmania* parasites to escape killing by neutrophil extracellular traps. Infect Immun. 2014;82(4):1732-40.

65. Carlsen ED, Liang Y, Shelite TR, Walker DH, Melby PC, Soong L. Permissive and protective roles for neutrophils in leishmaniasis. Clinical and Experimental Immunology. 2015;182(2):109-18.

66. Chaplin DD. Overview of the immune response. J Allergy Clin Immunol. 2010;125(2 Suppl 2):S3-23.

67. Sbarra AJ, Karnovsky ML. The biochemical basis of phagocytosis. I. Metabolic changes during the ingestion of particles by polymorphonuclear leukocytes. J Biol Chem. 1959;234(6):1355-62.

68. van Raam BJ, Verhoeven AJ, Kuijpers TW. Mitochondria in neutrophil apoptosis. Int J Hematol. 2006;84(3):199-204.

69. Injarabian L, Devin A, Ransac S, Marteyn BS. Neutrophil Metabolic Shift during their Lifecycle: Impact on their Survival and Activation. Int J Mol Sci. 2019;21(1).

70. O'Neill LA, Kishton RJ, Rathmell J. A guide to immunometabolism for immunologists. Nat Rev Immunol. 2016;16(9):553-65.

71. Gueirard P, Laplante A, Rondeau C, Milon G, Desjardins M. Trafficking of *Leishmania donovani* promastigotes in non-lytic compartments in neutrophils enables the subsequent transfer of parasites to macrophages. Cellular Microbiology. 2008;10(1):100-11.

72. Zandbergen Gv, Hermann N, Laufs H, Solbach W, Laskay T. *Leishmania* Promastigotes Release a Granulocyte Chemotactic Factor and Induce Interleukin-8 Release but Inhibit Gamma Interferon-Inducible Protein 10 Production by Neutrophil Granulocytes. Infection and Immunity. 2002;70(8):4177-84.

73. Aga E, Katschinski DM, van Zandbergen G, Laufs H, Hansen B, Müller K, et al. Inhibition of the Spontaneous Apoptosis of Neutrophil Granulocytes by the Intracellular Parasite *Leishmania major*. The Journal of Immunology. 2002;169(2):898-905.

74. van Zandbergen G, Klinger M, Mueller A, Dannenberg S, Gebert A, Solbach W, et al. Cutting Edge: Neutrophil Granulocyte Serves as a Vector for *Leishmania* Entry into Macrophages. The Journal of Immunology. 2004;173(11):6521-5.

75. Davies LC, Jenkins SJ, Allen JE, Taylor PR. Tissue-resident macrophages. Nature Immunology. 2013;14(10):986-95.

76. Wynn TA, Vannella KM. Macrophages in Tissue Repair, Regeneration, and Fibrosis. Immunity. 2016;44(3):450-62.

77. Chauhan P, Sarkar A, Saha B. Interplay Between Metabolic Sensors and Immune Cell Signaling. Exp Suppl. 2018;109:115-96.

78. Murray PJ, Wynn TA. Protective and pathogenic functions of macrophage subsets. Nature Reviews Immunology. 2011;11(11):723-37.

79. Martinez FO, Gordon S. The M1 and M2 paradigm of macrophage activation: time for reassessment. F1000Prime Rep. 2014;6:13.

80. Rodrigues V, Cordeiro-da-Silva A, Laforge M, Silvestre R, Estaquier J. Regulation of immunity during visceral *Leishmania* infection. Parasit Vectors. 2016;9:118.

81. Charan Raja MR, Srinivasan S, Subramaniam S, Rajendran N, Sivasubramanian A, Kar Mahapatra S. Acetyl shikonin induces IL-12, nitric oxide and ROS to kill intracellular parasite *Leishmania donovani* in infected hosts. RSC Advances. 2016;6(66):61777-83.

82. Panaro MA, Brandonisio O, Acquafredda A, Sisto M, Mitolo V. Evidences for iNOS expression and nitric oxide production in the human macrophages. Current drug targets Immune, endocrine and metabolic disorders. 2003;3(3):210-21.

83. Thapa B, Lee K. Metabolic influence on macrophage polarization and pathogenesis. BMB Rep. 2019;52(6):360-72.

84. Semba H, Takeda N, Isagawa T, Sugiura Y, Honda K, Wake M, et al. HIF-1α-PDK1 axis-induced active glycolysis plays an essential role in macrophage migratory capacity. Nat Commun. 2016;7:11635.

85. Ryan DG, O'Neill LAJ. Krebs cycle rewired for macrophage and dendritic cell effector functions. FEBS Letters. 2017;591(19):2992-3006.

86. Saunders EC, Ng WW, Kloehn J, Chambers JM, Ng M, McConville MJ. Induction of a stringent metabolic response in intracellular stages of *Leishmania mexicana* leads to increased dependence on mitochondrial metabolism. PLoS Pathog. 2014;10(1):e1003888.

87. Kloehn J, Saunders EC, O'Callaghan S, Dagley MJ, McConville MJ. Characterization of Metabolically Quiescent *Leishmania* Parasites in Murine Lesions Using Heavy Water Labeling. PLOS Pathogens. 2015;11(2):e1004683.

88. Saunders EC, Naderer T, Chambers J, Landfear SM, McConville MJ. *Leishmania mexicana* can utilize amino acids as major carbon sources in macrophages but not in animal models. Mol Microbiol. 2018;108(2):143-58.

89. Holzmuller P, Geiger A, Nzoumbou-Boko R, Pissarra J, Hamrouni S, Rodrigues V, et al. Trypanosomatid Infections: How Do Parasites and Their Excreted-Secreted Factors Modulate the Inducible Metabolism of l-Arginine in Macrophages? Front Immunol. 2018;9:778.

90. Aoki JI, Muxel SM, Zampieri RA, Laranjeira-Silva MF, Müller KE, Nerland AH, et al. RNA-seq transcriptional profiling of *Leishmania amazonensis* reveals an arginase-dependent gene expression regulation. PLoS Negl Trop Dis. 2017;11(10):e0006026.

91. Ilari A, Fiorillo A, Baiocco P, Poser E, Angiulli G, Colotti G. Targeting polyamine metabolism for finding new drugs against leishmaniasis: A review. Mini-Reviews in Medicinal Chemistry. 2015;15(3):243-52.

92. Rogers M, Kropf P, Choi BS, Dillon R, Podinovskaia M, Bates P, et al. Proteophosophoglycans regurgitated by *Leishmania*-infected sand flies target the L-arginine metabolism of host macrophages to promote parasite survival. PLoS Pathogens. 2009;5(8):e1000555.

93. Mandal A, Das S, Kumar A, Roy S, Verma S, Ghosh AK, et al. L-Arginine uptake by cationic amino acid transporter promotes intra-macrophage survival of *Leishmania donovani* by enhancing arginase-mediated polyamine synthesis. Frontiers in Immunology. 2017;8(JUL):839.

94. Goldman-Pinkovich A, Balno C, Strasser R, Zeituni-Molad M, Bendelak K, Rentsch D, et al. An Arginine Deprivation Response Pathway Is Induced in *Leishmania* during Macrophage Invasion. PLoS Pathogens. 2016;12(4):e1005494.

95. Aoki JI, Muxel SM, Laranjeira-Silva MF, Zampieri RA, Müller KE, Nerland AH, et al. Dual transcriptome analysis reveals differential gene expression modulation influenced by *Leishmania* arginase and host genetic background. Microb Genom. 2020;6(9):1-13.

96. Muxel SM, Mamani-Huanca M, Aoki JI, Zampieri RA, Floeter-Winter LM, López-Gonzálvez Á, et al. Metabolomic profile of BALB/c macrophages infected with *Leishmania amazonensis*: Deciphering L-arginine metabolism. International Journal of Molecular Sciences. 2019;20(24).

97. Reiner NE, Schultz LA, Malemud CJ. Eicosanoid metabolism by *Leishmania donovani*-infected macrophages: Mouse strain responses in prostanoid synthesis. American Journal of Tropical Medicine and Hygiene. 1988;38(1):59-64.

98. Ospina HA, Descoteaux A. *Leishmania donovani* modulates host macrophage mitochondrial metabolism, integrity, and function. Journal of Immunology. 2020;204(1).

99. Smirlis D, Dingli F, Pescher P, Prina E, Loew D, Rachidi N, et al. SILAC-based quantitative proteomics reveals pleiotropic, phenotypic modulation in primary murine macrophages infected with the protozoan pathogen *Leishmania donovani*. Journal of Proteomics. 2020;213:103617.

100. Gordon S, Martinez FO. Alternative activation of macrophages: mechanism and functions. Immunity. 2010;32(5):593-604.

101. Vats D, Mukundan L, Odegaard JI, Zhang L, Smith KL, Morel CR, et al. Oxidative metabolism and PGC-1beta attenuate macrophage-mediated inflammation. Cell Metab. 2006;4(1):13-24.

102. Ty MC, Loke P, Alberola J, Rodriguez A, Rodriguez-Cortes A. Immuno-metabolic profile of human macrophages after *Leishmania* and *Trypanosoma cruzi* infection. PLoS One. 2019; 14(12):e0225588.

103. Holzmuller P, Sereno D, Cavaleyra M, Mangot I, Daulouede S, Vincendeau P, et al. Nitric oxide-mediated proteasome-dependent oligonucleosomal DNA fragmentation in *Leishmania amazonensis* amastigotes. Infection and Immunity. 2002;70(7):3727-35.

104. Iniesta V, Gómez-Nieto LC, Corraliza I. The inhibition of arginase by Nω-hydroxy-L-arginine controls the growth *of Leishmania* inside macrophages. Journal of Experimental Medicine. 2001;193(6):777-83.

105. Ferreira C, Mesquita I, Barbosa AM, Osório NS, Torrado E, Beauparlant CJ, et al. Glutamine supplementation improves the efficacy of miltefosine treatment for visceral leishmaniasis. PLoS Neglected Tropical Diseases. 2020;14(3):e0008125.

106. Silva-Barrios S, Charpentier T, Stäger S. The Deadly Dance of B Cells with Trypanosomatids. Trends Parasitol. 2018;34(2):155-71.

107. Vallejo AN, Davila E, Weyand CM, Goronzy JJ. Biology of T lymphocytes. Rheum Dis Clin North Am. 2004;30(1):135-57.

108. Jawed JJ, Dutta S, Majumdar S. Functional aspects of T cell diversity in visceral leishmaniasis. Biomed Pharmacother. 2019;117:109098.

109. Costa-Madeira JC, Trindade GB, Almeida PHP, Silva JS, Carregaro V. T Lymphocyte Exhaustion During Human and Experimental Visceral Leishmaniasis. Front Immunol. 2022;13:835711.

110. Jawed JJ, Banerjee S, Bandyopadhyay S, Parveen S, Chowdhury BP, Saini P, et al. Immunomodulatory effect of Arabinosylated lipoarabinomannan restrict the progression of visceral leishmaniasis through NOD2 inflammatory pathway: Functional regulation of T cell subsets. Biomed Pharmacother. 2018;106:724-32.

111. Ikeogu NM, Edechi CA, Akaluka GN, Feiz-Barazandeh A, Zayats RR, Salako ES, et al. Semaphorin 3E Promotes Susceptibility to *Leishmania major* Infection in Mice by Suppressing CD4(+) Th1 Cell Response. J Immunol. 2021;206(3):588-98.

112. Rostan O, Gangneux JP, Piquet-Pellorce C, Manuel C, McKenzie AN, Guiguen C, et al. The IL-33/ST2 axis is associated with human visceral leishmaniasis and suppresses Th1 responses in the livers of BALB/c mice infected with *Leishmania donovani*. mBio. 2013;4(5):e00383-13.

113. Sacramento LA, Cunha FQ, de Almeida RP, da Silva JS, Carregaro V. Protective role of 5-lipoxigenase during *Leishmania infantum* infection is associated with Th17 subset. Biomed Res Int. 2014; 2014:264270.

114. Nascimento MSL, Carregaro V, Lima-Júnior DS, Costa DL, Ryffel B, Duthie MS, et al. Interleukin 17A Acts Synergistically With Interferon γ to Promote Protection Against *Leishmania infantum* Infection. The Journal of Infectious Diseases. 2014;211(6):1015-26.

115. Sacramento LA, da Costa JL, de Lima MH, Sampaio PA, Almeida RP, Cunha FQ, et al. Toll-Like Receptor 2 Is Required for Inflammatory Process Development during *Leishmania infantum* Infection. Front Microbiol. 2017;8:262.

116. Scott P, Natovitz P, Coffman RL, Pearce E, Sher A. Immunoregulation of cutaneous leishmaniasis. T cell lines that transfer protective immunity or exacerbation belong to different T helper subsets and respond to distinct parasite antigens. J Exp Med. 1988;168(5):1675-84.

117. Thakur CP, Mitra DK, Narayan S. Skewing of cytokine profiles towards T helper cell type 2 response in visceral leishmaniasis patients unresponsive to sodium antimony gluconate. Trans R Soc Trop Med Hyg. 2003;97(4):409-12.

118. Carneiro MB, Lopes ME, Hohman LS, Romano A, David BA, Kratofil R, et al. Th1-Th2 Cross-Regulation Controls Early *Leishmania* Infection in the Skin by Modulating the Size of the Permissive Monocytic Host Cell Reservoir. Cell Host Microbe. 2020;27(5):752-68.e7.

119. Michalek RD, Gerriets VA, Jacobs SR, Macintyre AN, MacIver NJ, Mason EF, et al. Cutting edge: distinct glycolytic and lipid oxidative metabolic programs are essential for effector and regulatory $CD4^+$ T cell subsets. J Immunol. 2011;186(6):3299-303.

120. Shi LZ, Wang R, Huang G, Vogel P, Neale G, Green DR, et al. HIF1alpha-dependent glycolytic pathway orchestrates a metabolic checkpoint for the differentiation of TH17 and Treg cells. J Exp Med. 2011;208(7):1367-76.

121. Liu R-T, Zhang M, Yang C-L, Zhang P, Zhang N, Du T, et al. Enhanced glycolysis contributes to the pathogenesis of experimental autoimmune neuritis. Journal of Neuroinflammation. 2018;15(1):51.

122. Chang CH, Curtis JD, Maggi LB, Jr., Faubert B, Villarino AV, O'Sullivan D, et al. Posttranscriptional control of T cell effector function by aerobic glycolysis. Cell. 2013;153(6):1239-51.

123. Stark JM, Tibbitt CA, Coquet JM. The Metabolic Requirements of Th2 Cell Differentiation. Front Immunol. 2019;10:2318.

124. Rai AK, Thakur CP, Singh A, Seth T, Srivastava SK, Singh P, et al. Regulatory T cells suppress T cell activation at the pathologic site of human visceral leishmaniasis. PLoS One. 2012;7(2):e31551.

125. Leveque L, Deknuydt F, Bioley G, Old LJ, Matsuzaki J, Odunsi K, et al. Interleukin 2-mediated conversion of ovarian cancer-associated $CD4^+$ regulatory T cells into proinflammatory interleukin 17-producing helper T cells. J Immunother. 2009;32(2):101-8.

126. Jawed JJ, Majumder S, Bandyopadhyay S, Biswas S, Parveen S, Majumdar S. SLA-PGN-primed dendritic cell-based vaccination induces Th17-mediated protective immunity against experimental visceral leishmaniasis: a crucial role of PKCβ. Pathog Dis. 2016;74(5).

127. Wherry EJ, Teichgräber V, Becker TC, Masopust D, Kaech SM, Antia R, et al. Lineage relationship and protective immunity of memory CD8 T cell subsets. Nat Immunol. 2003;4(3):225-34.

128. Gubser PM, Bantug GR, Razik L, Fischer M, Dimeloe S, Hoenger G, et al. Rapid effector function of memory $CD8^+$ T cells requires an immediate-early glycolytic switch. Nat Immunol. 2013; 14(10):1064-72.

129. Moreira D, Rodrigues V, Abengozar M, Rivas L, Rial E, Laforge M, et al. *Leishmania infantum* modulates host macrophage mitochondrial metabolism by hijacking the SIRT1-AMPK axis. PLoS Pathog. 2015;11(3):e1004684.

130. Koivunen P, Kietzmann T. Hypoxia-Inducible Factor Prolyl 4-Hydroxylases and Metabolism. Trends Mol Med. 2018;24(12):1021-35.

131. Xie Y, Shi X, Sheng K, Han G, Li W, Zhao Q, et al. PI3K/Akt signaling transduction pathway, erythropoiesis and glycolysis in hypoxia (Review). Mol Med Rep. 2019;19(2):783-91.

132. Ersahin T, Tuncbag N, Cetin-Atalay R. The PI3K/AKT/mTOR interactive pathway. Mol Biosyst. 2015;11(7):1946-54.

133. Thomas SA, Nandan D, Kass J, Reiner NE. Countervailing, time-dependent effects on host autophagy promotes intracellular survival of *Leishmania*. Journal of Biological Chemistry. 2018;293(7):2617-30.

134. Mesquita I, Ferreira C, Moreira D, Kluck GEG, Barbosa AM, Torrado E, et al. The Absence of HIF-1alpha Increases Susceptibility to *Leishmania donovani* Infection via Activation of BNIP3/mTOR/SREBP-1c Axis. Cell Rep. 2020;30(12):4052-64.e7.

135. Rabhi I, Rabhi S, Ben-Othman R, Rasche A, Daskalaki A, Trentin B, et al. Transcriptomic Signature of *Leishmania* Infected Mice Macrophages: A Metabolic Point of View. PLoS Neglected Tropical Diseases. 2012;6(8):e1763.

136. Galluzzi L, Diotallevi A, De Santi M, Ceccarelli M, Vitale F, Brandi G, et al. *Leishmania infantum* induces mild unfolded protein response in infected macrophages. PLoS ONE. 2016; 11(12):e0168339.

137. Cantó C, Gerhart-Hines Z, Feige JN, Lagouge M, Noriega L, Milne JC, et al. AMPK regulates energy expenditure by modulating NAD^+ metabolism and SIRT1 activity. Nature. 2009;458(7241):1056-60.

138. Ohms M, Ferreira C, Busch H, Wohlers I, Guerra de Souza AC, Silvestre R, et al. Enhanced Glycolysis Is Required for Antileishmanial Functions of Neutrophils Upon Infection With *Leishmania donovani*. Front Immunol. 2021;12:632512.

139. Reimão JQ, Pita Pedro DP, Coelho AC. The preclinical discovery and development of oral miltefosine for the treatment of visceral leishmaniasis: a case history. Expert Opin Drug Discov. 2020;15(6):647-58.

140. Moreira D, Santarém N, Loureiro I, Tavares J, Silva AM, Amorim AM, et al. Impact of continuous axenic cultivation in *Leishmania infantum* virulence. PLoS Negl Trop Dis. 2012;6(1):e1469.

141. Lin G-J, Sytwu H-K, Yu J-C, Chen Y-W, Kuo Y-L, Yu C-C, et al. Dimethyl sulfoxide inhibits spontaneous diabetes and autoimmune recurrence in non-obese diabetic mice by inducing differentiation of regulatory T cells. Toxicology and Applied Pharmacology. 2015;282(2):207-14.

142. Jain SK, Sahu R, Walker LA, Tekwani BL. A parasite rescue and transformation assay for antileishmanial screening against intracellular *Leishmania donovani* amastigotes in THP1 human acute monocytic leukemia cell line. J Vis Exp. 2012(70).

143. Faria J, Barbosa J, Queirós O, Moreira R, Carvalho F, Dinis-Oliveira RJ. Comparative study of the neurotoxicological effects of tramadol and tapentadol in SH-SY5Y cells. Toxicology. 2016;359-360:1-10.

144. Livak KJ, Schmittgen TD. Analysis of relative gene expression data using real-time quantitative PCR and the 2(-Delta Delta C(T)) Method. Methods. 2001;25(4):402-8.

145. Cai R, Zhang Y, Simmering JE, Schultz JL, Li Y, Fernandez-Carasa I, et al. Enhancing glycolysis attenuates Parkinson's disease progression in models and clinical databases. J Clin Invest. 2019;129(10):4539-49.

146. Hong CT, Chau KY, Schapira AH. Meclizine-induced enhanced glycolysis is neuroprotective in Parkinson disease cell models. Sci Rep. 2016;6:25344.

147. Gohil VM, Sheth SA, Nilsson R, Wojtovich AP, Lee JH, Perocchi F, et al. Nutrient-sensitized screening for drugs that shift energy metabolism from mitochondrial respiration to glycolysis. Nature Biotechnology. 2010;28(3):249-55.

148. Kamperdijk EWA, Verdaasdonk MAM, Beelen RHJ. Expression and Function of MHC Class II Antigens on Macrophages and Dendritic Cells. In: Fossum S, Rolstad B, editors. Histophysiology of the Immune System: The Life History, Organization, and Interactions of Its Cell Populations. Boston, MA: Springer US; 1988. p. 789-93.

149. Orecchioni M, Ghosheh Y, Pramod AB, Ley K. Macrophage Polarization: Different Gene Signatures in M1(LPS$^+$) vs. Classically and M2(LPS$^-$) vs. Alternatively Activated Macrophages. Front Immunol. 2019;10:1084.

150. Shook B, Xiao E, Kumamoto Y, Iwasaki A, Horsley V. CD301b$^+$ Macrophages Are Essential for Effective Skin Wound Healing. Journal of Investigative Dermatology. 2016;136(9):1885-91.

151. de Melo Mendes V, Tempone AG, Treiger Borborema SE. Antileishmanial activity of H1-antihistamine drugs and cellular alterations in *Leishmania (L.) infantum*. Acta Tropica. 2019;195:6-14.

152. Gao L, Wang C, Qin B, Li T, Xu W, Lenahan C, et al. 6-phosphofructo-2-kinase/fructose-2,6-bisphosphatase Suppresses Neuronal Apoptosis by Increasing Glycolysis and "cyclin-dependent

kinase 1-Mediated Phosphorylation of p27 After Traumatic Spinal Cord Injury in Rats. Cell Transplant. 2020;29:963689720950226.

153. Pinto EG, da Costa-Silva TA, Tempone AG. Histamine H1-receptor antagonists against Leishmania *(L.) infantum*: An *in vitro and in vivo* evaluation using phosphatidylserine-liposomes. Acta Tropica. 2014;137:206-10.

154. Kishi S, Campanholle G, Gohil VM, Perocchi F, Brooks CR, Morizane R, et al. Meclizine Preconditioning Protects the Kidney Against Ischemia-Reperfusion Injury. EBioMedicine. 2015;2(9):1090-101.

155. Gohil VM, Zhu L, Baker CD, Cracan V, Yaseen A, Jain M, et al. Meclizine inhibits mitochondrial respiration through direct targeting of cytosolic phosphoethanolamine metabolism. J Biol Chem. 2013;288(49):35387-95.

156. Guan Y, Chen X, Wu M, Zhu W, Arslan A, Takeda S, et al. The phosphatidylethanolamine biosynthesis pathway provides a new target for cancer chemotherapy. J Hepatol. 2020;72(4):746-60.

157. Pérez-Cabezas B, Cecílio P, Gaspar TB, Gärtner F, Vasconcellos R, Cordeiro-da-Silva A. Understanding Resistance vs. Susceptibility in Visceral Leishmaniasis Using Mouse Models of *Leishmania infantum* Infection. Front Cell Infect Microbiol. 2019;9:30.

158. Mukherjee M, Basu Ball W, Das PK. *Leishmania donovani* activates SREBP2 to modulate macrophage membrane cholesterol and mitochondrial oxidants for establishment of infection. Int J Biochem Cell Biol. 2014;55:196-208.

159. Parmar N, Chandrakar P, Kar S. *Leishmania donovani* Subverts Host Immune Response by Epigenetic Reprogramming of Macrophage M(Lipopolysaccharides + IFN-γ)/M(IL-10) Polarization. J Immunol. 2020;204(10):2762-78.

160. Gomes-Alves AG, Maia AF, Cruz T, Castro H, Tomás AM. Development of an automated image analysis protocol for quantification of intracellular forms of *Leishmania spp.* PLoS One. 2018; 13(8):e0201747.

161. Moraes CB, Alcântara LM. Quantification of Parasite Loads by Automated Microscopic Image Analysis. Methods Mol Biol. 2019;1971:279-88.

162. Zhang H, Ma J, Tang K, Huang B. Beyond energy storage: roles of glycogen metabolism in health and disease. Febs j. 2021;288(12):3772-83.

163. Samuel VT, Shulman GI. The pathogenesis of insulin resistance: integrating signaling pathways and substrate flux. J Clin Invest. 2016;126(1):12-22.

164. Rabinowitz JD, Enerbäck S. Lactate: the ugly duckling of energy metabolism. Nat Metab. 2020;2(7):566-71.

165. Plitzko B, Loesgen S. Measurement of Oxygen Consumption Rate (OCR) and Extracellular Acidification Rate (ECAR) in Culture Cells for Assessment of the Energy Metabolism. Bio Protoc. 2018;8(10):e2850.

166. Østerud B, Olsen JO. Pro- and anti-inflammatory effects of histamine on tissue factor and TNFα expression in monocytes of human blood. Thromb Res. 2014;133(3):477-80.

167. Chen S, Luster AD. Antihistamines for cancer immunotherapy: More than just treating allergies. Cancer Cell. 2022;40(1):9-11.

168. Li H, Xiao Y, Li Q, Yao J, Yuan X, Zhang Y, et al. The allergy mediator histamine confers resistance to immunotherapy in cancer patients via activation of the macrophage histamine receptor H1. Cancer Cell. 2022;40(1):36-52.e9.

169. Marone G, Granata F, Spadaro G, Genovese A, Triggiani M. The histamine-cytokine network in allergic inflammation. J Allergy Clin Immunol. 2003;112(4 Suppl):S83-8.

170. Peng R, Zhang W, Zuo Z, Shan Y, Liu X, Tang Y, et al. Dimethyl sulfoxide, a potent oral radioprotective agent, confers radioprotection of hematopoietic stem and progenitor cells independent of apoptosis. Free Radical Biology and Medicine. 2020;153:1-11.

ANNEX

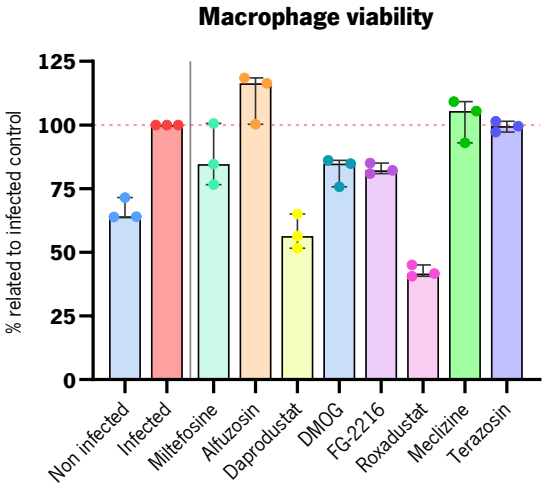

Sup. Figure 1. Alfuzosin, Meclizine and Terazosin treatments applied at 7h post-infection did not interfere with macrophage viability. The infected BMDMs viability after treatment was assessed on the 4th day post-infection through the Sulforhodamine B assay. The applied Friedman showed a statistically significant difference in macrophage viability between the different applied treatments, $X^2(9) = 24.53$, $p = 0.004$.